POLITECNICO DI MILANO

Department of Electronics, Information and Bioengineering Master of
Science in Biomedical Engineering

POLITECNICO
MILANO 1863

Advanced Virtual Reality Interface for

Navigated Prostate Biopsy

Supervisor: Giancarlo FERRIGNO, PhD

Co-Supervisor: Elena DE MOMI, PhD

Foreign Advisor: Cristian LUCIANO, PhD

Master Thesis of

Lorenzo RAPETTI

Student ID: 858899

Academic Year 2016-2017

To my family,
and my friends.

SOMMARIO

Il tumore alla prostata è la forma più comune di tumore non-cutaneo. La diagnosi del tumore viene fatta tramite test di screening non invasivi, ma un risultato positivo deve essere confermato attraverso una biopsia alla prostata. Durante la biopsia, secondo la procedura detta "sistematica", il chirurgo preleva circa 12 campioni di tessuto in modo casuale sotto la guida di un ecografo transrettale utilizzato per determinare la posizione della prostata. Recentemente, sono state introdotte alcune tecniche di fusione tra immagini ecografiche e MRI pre-operatorie, al fine di effettuare una biopsia "targeted" e riuscendo in questo modo a limitare il numero di campioni ad una area sospetta. Dal momento che l'ecografo deforma la prostata durante la procedura, le immagini MRI pre-operative non corrispondono all'anatomia del paziente, ed è quindi necessario l'utilizzo di complessi algoritmi di deformazione delle immagini MRI. Tuttavia, nonostante questo incremento nella complessità e nei costi, non c'è evidenza scientifica che le tecniche di fusione di ultrasound e MRI possano effettivamente migliorare l'accuratezza e i risultati chirurgici.

Questa tesi presenta un innovativo sistema di navigazione chirurgica per effettuare una biopsia "targeted" alla prostata senza il fastidio dato dalla sonda ecografica. Il sistema prevede che un tracker elettromagnetico tracci costantemente sia l'ago che il paziente in modo da fornirne costantemente posizione ed orientamento 3D. Alcuni marker vengono posizionati sulla pelle del paziente (in corrispondenza della cresta iliaca e dell'osso pubico) durante l'acquisizione di immagini MR, e vengono utilizzati per realizzare registrazione dell'immagine volumetrica MRI e il sistema di coordinate del tracker. Queste informazioni vengono quindi passate al sistema di navigazione che guida il chirurgo all'inserimento dell'ago nel perineo, e attraverso gli strati anatomici, fino ad arrivare al target. Una volta che il paziente viene portato in sala operatoria, vengono quindi fornite al chirurgo: un'interfaccia stereoscopica 3D, le viste ortogonali delle immagini MR, e la relativa posizione dell'ago.

Il principale contributo di questo lavoro è stata l'implementazione di un prototipo per questa procedura, focalizzando l'attenzione alla comunicazione tra il sistema di tracking e l'interfaccia grafica. Lo sviluppo di questa applicazione è stato possibile grazie alla creazione di una piattaforma in grado di fornire gli elementi base per l'implementazione di applicazioni basate su virtual reality e mixed reality. La piattaforma è stata chiamata *LACE*

library, e consiste in un SDK intuitivo, che unisce una grafica ad alte performance, con il tracking e l'aptica.

L'applicazione è stata sviluppata sotto la supervisione di alcuni chirurghi esperti della University of Illinois at Chicago e dell'ospedale Sacco di Milano, e l'interfaccia è stata testata con successo da studenti di medicina dell'Università degli Studi di Milano.

SUMMARY

Prostate cancer is the most common non-cutaneous cancer. Tumor detection involves non-invasive screening tests, but positive results must be confirmed by a prostate biopsy. About twelve random samples are obtained during the biopsy, which is a systematic procedure traditionally performed with trans-rectal ultrasound (TRUS) guidance to determine prostate location. Recently, methods of fusion between TRUS and preoperative MRI have been introduced in order to perform targeted biopsies aimed to reduce the number of samples to few suspicious areas. Since the TRUS displaces the prostate during the procedure, the preoperative MRI does not match patient anatomy. Therefore, complex MRI deformation algorithms are needed. However, despite the substantial increase in complexity and cost, there is no strong evidence that the TRUS-MRI fusion actually improves accuracy and surgical outcomes.

This thesis presents an innovative virtual reality surgical navigation system for performing targeted prostate biopsies, without the need of the uncomfortable TRUS. Both biopsy needle and patient anatomy are constantly tracked by an electromagnetic tracking system that provides their 3D position and orientation with respect to the surgical bed. Multiple fiducial markers are placed on the patient skin (at the iliac crest and pubic bone) during MRI scanning. Once in the operative room, the surgeon is presented a stereoscopic 3D volumetric rendering and multiple orthogonal views of the patient anatomy, as well as a virtual representation of the tracked needle. After a simple registration process between the MRI and the tracker coordinate system, the navigation system guides the needle insertion in the patient perineum through several anatomical layers towards the biopsy targets in the prostate.

The main contribution of this work is the implementation of a prototype for this procedure, focused on the integration between the tracking system and a graphics interface. The development of such an application has been possible thanks to the creation of a platform able to provide all the basic elements that allow to implement virtual/mixed reality based applications. The platform is called *LACE library,* and consists of an intuitive software development kit that conjugate high-performance graphics, tracking and haptics.

The application has been developed guided by expert surgeons of University of Illinois at Chicago and Sacco hospital at Milan, and the interface has been successfully tested by medical students at Università degli Studi di Milano.

ACKNOWLEDGMENTS

TABLE OF CONTENTS

x

LIST OF FIGURES

LIST OF TABLES

LIST OF ABBREVIATIONS

AS	Ascension 3D Guidance®
AR	Augmented Reality
BPH	Benign Prostatic Hyperplasia
DoF	Degrees of Freedom
DWI	Diffusion-Weighted Imaging
DRE	Digital Rectal Examination
DCE	Dynamic Contrast-Enhanced Imaging
EMTS	Electromagnetic Tracking System
FDA	Food and Drug Administration
GUI	Graphical User Interface
LUTS	Lower Urinary Tract Symptoms
MRI	Magnetic Resonance Imaging
MRSI	Magnetic Resonance Spectroscopy Imaging
mp-MRI	Multi-Parametric Magnetic Resonance Imaging
NDI	Northern Digital Incorporated
PDU	Power Doppler Ultrasound
PBx	Prostate Biopsy
PCa	Prostate Cancer
CZ	Prostate Central Zone
PZ	Prostate Peripheral Zone
PSA	Prostate-Specific Antigen
TZ	Prostate Transition Zone
QH	QuickHaptics$^{\text{TM}}$

SDK	Software Development Kit
STPB	Stereotactic Transperineal Prostate Biopsy
T1WI	T1-Weighted Imaging
T2WI	T2-Weighted Imaging
TRUS	Transrectal Ultrasound
UIC	University of Illinois at Chicago
US	Ultrasound
VR	Virtual Reality
VRPBx	Virtual Reality Navigation System for Prostate Biopsy
VL	Visualization Library
WK	Wykobi Computational Geometry Library
2D	2-Dimensional
3D	3-Dimensional

1 INTRODUCTION

The prostate cancer (PCa) is an abnormal growth of cells in the prostate gland; it is the most common non-cutaneous cancer in man. The most recent statistics available for the United States report 176,450 diagnoses of PCa and 27,681 cases of death in the 2013[1]. For 2016 the estimates of the American Cancer Society are about 180,890 new cases and about 26,120 deaths from PCa[2]. Screening and early detection are key factors for the therapy of the cancer in order to have better patient outcomes. The PCa screening involves the prostate-specific antigen (PSA) blood test and the digital rectal exam (DRE), but none of the existing tests is 100% accurate and an abnormal result need a prostate biopsy (PBx) to determine the presence of cancer. The PBx is the most accurate way to evaluate the suspicious cells inside the prostate gland; it consists in taking multiple samples from patient prostate to investigate under a microscope whether or not cancerous cells are present, and to determine an appropriate treatment according to the stage of the cancer. The most common procedure (12-core transrectal PBx) consist in using a hollow needle that is inserted through the rectum to take 12 samples from different areas of the prostate under the guidance of real-time images provided by a transrectal ultrasound (TRUS). Despite this technique is considered as the "gold standard", the absence of real-time images of tumor leads to sampling errors, unnecessary high number of samples and false negative results[3], moreover the presence of the TRUS increase the discomfort for the patient and the occurrence of complications. Recently, integrating TRUS imaging with multiparametric magnetic resonance imaging (mp-MRI), new methods for targeted biopsy have been developed. The guidance of MRI-TRUS fusion allows the surgeon to limit the number of samples taken, the performance time and the risks for the patient, and an higher accuracy can be achieved[4].

However, the TRUS is still present in all the PBx clinical set-ups; the ultrasound (US) probe, in addiction to be a cause of pain and discomfort for the patient, it causes tissues displacement increasing the complexity of the MRI-TRUS images registration.

Over the past decade, navigation techniques in surgery have evolved, thanks to improved computer technologies and imaging methods, safer and less invasive procedures have been introduced[5]. The first discipline to widely adopt computer virtual image-guided techniques is Neurosurgery, presenting good clinical results over the standard procedures. In virtual image-based navigation systems pre-operative images are registered to the patient position and the instrument is tracked, fusing the two information the instrument can be visualized in the same "virtual coordinate system" of the images in real-time. One example of the application of this technique in neurosurgery is the frame-less stereotactic surgery for brain biopsy that aims to replace physical frame of reference with virtual images, the performance of this method has been tested to be comparable to the one of the frame-based procedure[6].

Given the neurosurgery examples and the weakness of PBx navigation techniques, I have been involved in a project that proposes and evaluate the use of up-to-date technologies in order to implement a *Virtual Reality Navigation System for Prostate Biopsy* that can improve the accuracy and safety of the procedure replacing the TRUS real-time guidance with an electromagnetic tracking system (EMTS). The project is the result of the collaboration between University of Illinois at Chicago (UIC) and Politecnico di Milano; in particular, it has been conducted respectively at the Mixed Reality Lab at UIC and the Nearlab (Neuroengineering and Medical Robotics Lab) at Politecnico di Milano.

At the Mixes Reality Lab, the first experimental set-up has been developed and tested thanks to the help of expert urologist. The project was then continued in Milano where a second experimental set-up has been implemented, and it has been used to collect evaluation data on the graphics interface offered by the application.

In the following chapters, it is explained how the system has been conceived starting from the problem identification, through the implementation, up to the testing of the application interface. Besides the *Virtual Reality Navigation System*, the document presents also the *LACE library*, a software development kit (SDK) that has been developed in parallel to the application.

2 BACKGROUND[1]

2.1 PROSTATE: CLINICAL ASPECT

The prostate is a gland located in the men pelvis that takes part in urinary flow control and in male reproductive system. It has a high oncological relevance since it is the non-cutaneous tissue with the highest incidence of cancer.

In the first part of this section an overview of anatomy and physiology of the prostate is presented. In the second part the PCa will be discussed presenting all the process from the detection to the therapy.

2.1.1 PROSTATE PHYSIOLOGY

Anatomy

The prostate is a composite organ found in men sub peritoneal compartment anterior to the rectum and between the bladder and the penis[7] (see Figure 1). The prostate shape is described in the literature as a "walnut", and a normal prostate weights approximately 20g and it is 3cm in length, 4cm in wide and 2cm in depth[8], but the dimension can vary due to aging (BPH) or pathology (PCa). The prostate is composed of glandular elements and

---

[1] This chapter has been partially taken from the works of the author at [66][67]

stromal elements encapsulated in a collagen and elastin layer, and surrounded by smooth muscles.

Male-typical reproductive anatomy
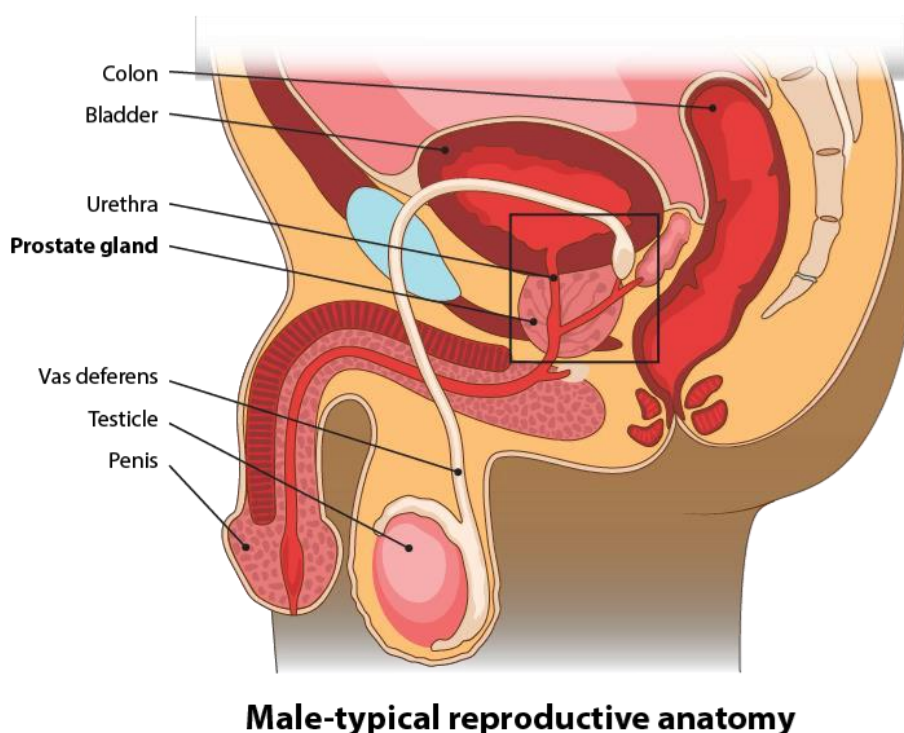
Figure 1: Anatomy of the Male Reproductive and Urinary System
The prostate gland is at the center of the image located below the bladder, above the penis and anterior to the rectum. The prostate is crossed by the urethra that flows from the bladder, and the ejaculatory ducts running from the seminal vesicles.
(Image courtesy of Katja Tetzlaff)

The prostate gland is divided in three zones with different embryologic origins and different functions. The zones of the prostate, as shown in Figure 2, are:

- Peripheral Zone (PZ)

The PZ is closest zone to the rectum and it is the largest zone of the prostate in a healthy subject. Because of its location, it is possible for a doctor to palpate this area through a digital rectal examination (DRE).

- Transition Zone (TZ)

The TZ is located in between the other two zones and it is crossed by the urethra as it passes through the prostate. The benign prostatic hyperplasia (BPH) happen in this area, it is caused by the proliferation of muscle cells that causes an enlargement which can

cause the movement of the PZ towards the rectum and can push the urethra causing lower urinary tract symptoms (LUTS)[9].

- Central Zone (CZ)

The CZ is the more distant zone from the rectum and the ejaculatory ducts cross it. Because of its location, this area cannot be felt during a DRE.
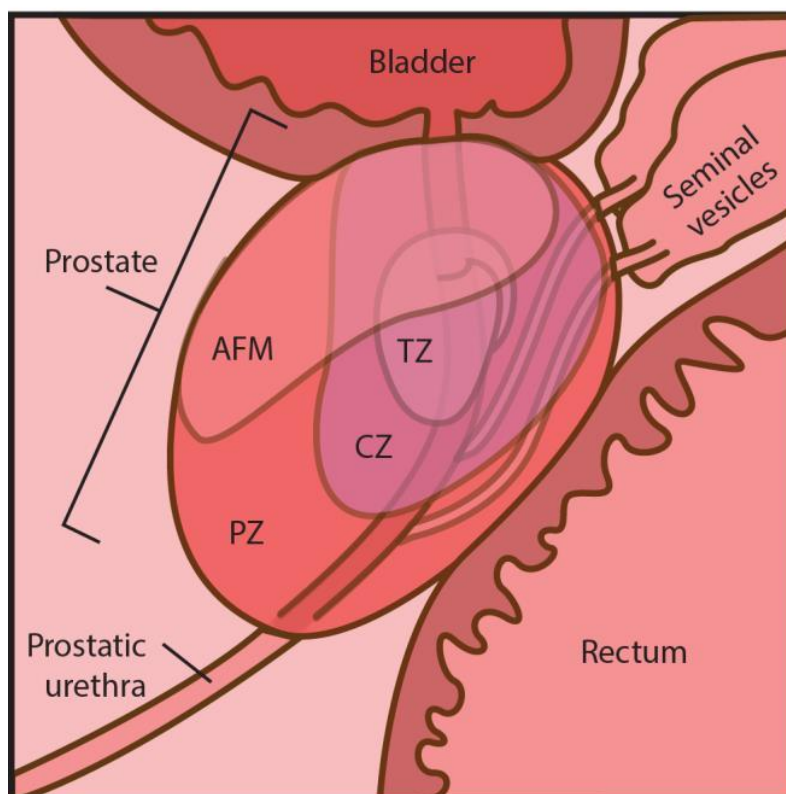
Figure 2: Zones of the Prostate Gland
The transitional zone and central zone are the central portions, the first one is crossed only by the urethra, while in the central zone the ejaculatory ducts flow into the urethra. The peripheral zone constitute the bigger portion of the prostate and it is the closest one to the rectum.
(*Image courtesy of Katja Tetzlaff*)

Function

The prostate takes part both in the male reproductive and urinary system.

The prostate is responsible for the secretion the fluid portion of semen volume containing proteins and simple sugars that have the function of maintain and nourish sperm cell[10]. The sperm runs from the seminal vesicles through the ejaculatory duct that crosses the CZ of the prostate, this duct empty into the urethra so that the semen can leave the body during orgasm.

The prostate plays a role also in controlling urinary flow, the urinary tract starts from the bladder and crosses the TZ of the prostate before reaching the penis, and prostate muscles are wrapped around this channel. The contraction of those muscular fibers can regulate the flow inside the urethra.

2.1.2 PROSTATE CANCER

The PCa is an abnormal growth of cells in the prostate and it is the most common non-cutaneous cancer in man, recent statistics available for the United States report 27,681 cases of death in the 2013[1]. For 2016 the estimates of the American Cancer Society (ACS) are about 180,890 new cases and about 26,120 deaths from PCa[2].

Most of the PCa are adenocarcinomas developed in the gland cells, according to statistics about 70% of PCa arise from the PZ, 25% form TZ and 5% from the CZ[7]. Furthermore, researches have showed that, with percentage between 60%-90%, PCa develops as multifocal cancer (it is found in different sites of the gland) that implies complexity in prognosis and therapy[11].

Detection

Screening and early detection are key factors for the therapy of the cancer in order to have better patient outcomes. During the early stage the PCa does not cause any symptoms, but as the tumor grow it cause the prostate to swell leading to disturb during urination and ejaculation. When the tumor reach an advanced stage the subject can experience more symptoms such as pain in the pelvis, nausea, loss of weight, and weakness in the lower limb[12].

The early screening for PCa involves three main exams: the PSA test, the DRE and mp-MRI.

- DRE

The DRE is an exam, performed by a doctor, which consists in putting a gloved finger inside the patient rectum to check the dimension of the prostate[13]. This technique allows the doctor to feel the presence of abnormal enlargement close to the rectal wall in correspondence of the posterior portion of the gland, which is the region more affected by the pathology. The abnormal growth that can be felt is usually located in the PZ and eventually in the TZ, while an abnormal growth in the CZ cannot be felt. For the DRE alone, the measured values of sensitivity in detecting PCa is 37%, while the value of specificity is 91%[14]. The low value of sensitivity is due to the fact that this technique cannot detect small tumors and those tumors that are located far from the posterior part of the prostate.

- PSA exam

PSA is a serine protease secreted both by prostate gland epithelial cells and PCa cells. In healthy subjects it can be found in the semen and in low level in other fluids such as urine and blood. Different studies have been conducted on PSA to evaluate the relation between PSA and PCa, in 1994 the PSA test has been approved by the Food and Drug Administration (FDA) as an early detection exam for the PCa in conjunction with DRE[15]. The test consists in the measure of PSA level in the blood. The standard threshold for the PSA test is 4 ng/ml with a sensitivity over 85% and a specificity of 33%. The high presence of false positive is due to the fact that PSA level can fluctuate for many causes (such as prostatesis or urinary tract infection) and vary in between different populations (different age or ethnic groups)[16]. PCa standard screening is done using PSA exam in combined with DRE.

- TRUS

PCa can appear in US images as hyperechoic lesion. Anyway, most of PCa are not visible with TRUS (between 40% and 60%), and about 50% of the visible hypercolic areas are not cancer[17]. Currently, the TRUS is more used as guidance during therapy and PBx than as a screening technique, but its role could gain importance in tumor detection and localization thanks to new technique such as US elastography, Power Doppler Ultrasound (PDU) and contrast enhanced US[18]. A review of those techniques is presented in chapter 2.2.

- mp-MRI

The information of MRI is used for the detection, characterization and staging of PCa in order to determine treatment strategies. In particular, MRI is used as for biopsy guidance and during radical prostatectomy preoperative stages[19]. Currently, the used MRI scanner works both with 1.5 and 3.0 Tesla, and an endorectal coil can be used in order to reduce noise. Different techniques of mp-MRI, with different parameters, have been studied; the most common techniques are the following:

- T1-Weighted Imaging (T1WI)

The contrast provided by T1WI for the prostate gland is generally small. T1WI finds a more spread application in detecting eventual hemorrhages consequent to PBx[20].

- T2-Weighted Imaging (T2WI)

T2WI provides a good spatial resolution and contrast for the depiction of PZ and CZ of the prostate; therefore, tumors in those regions may appear well defined. However, against a good sensitivity (about 80%), the detection specificity is low (about 50%) since other pathologies (such as BPH) cause similar signals[21].

- Diffusion-Weighted Imaging (DWI)

DWI is an MR technique based on the measurement of water diffusion[22]. A PCa is a region with high density of glandular elements, so it can be identified in DWI as a region with lower water displacement. From literature, the measured interval of sensitivity and specificity range respectively in 74%-83% and 50%-81%[21].

- Dynamic Contrast-Enhanced Imaging (DCE)

DCE uses high time resolution T1WI to measure the flow of a contrast material in the prostate. The measured signal can be used to evaluate the vascular properties of the tissue; regions with higher vascularity may be caused by the presence of PCa (other causes can be BPH or inflammation). Measured values of sensitivity and Specificity in DCE are respectively 74% are 81% [20].

- Magnetic resonance spectroscopy imaging (MRSI)

MRSI is an imaging technique that can provide prostate metabolic information. The performance of this technique is higher than other image techniques both in term of

sensitivity (95%) and specificity (91%), but it requires a more complex measurement system.

Although many techniques for the detection and staging of PCa have been presented, none of them is 100% accurate, to this day, the biopsy is the most accurate way to evaluate the suspicious cells inside the prostate gland. For this reason, abnormal screening test requires a PBx, which is the only way to determine the presence of cancer and proceed with the most effective therapy.

PBx is a procedure that consists in using a hollow needle to take a number of samples from the patient prostate tissue. The samples will be then analyzed under the microscope in order to determine the presence of cancerous cells[13]. A more detailed description of the PBx procedure is provided in section 2.2.

Therapy

After the detection of PCa, many different solutions can be carried on; the choice of the therapy depends on patient anagraphic data, clinical history and on the information provided by medical images. Currently, the available options are the following[13]:

- Active Surveillance

One option can be not to start a therapy, but to wait to see how and if the tumor is going to grow and spread. This can be done because sometimes the tumor grows slowly without causing symptoms.

- Prostatectomy

The prostatectomy is a surgery procedure that consists in removing part of the prostate or, more often, the totality of the prostate (Radical prostatectomy). For this surgical procedure the laparoscopic robotic approach is spread, and it is preferred to open surgery[23].

- Radiation Treatment (Brachytherapy)

This treatment involves the use of high-energy ionizing radiation to kill the cancerous cells.

- Hormone Therapy

This therapy consists in reducing the number of those hormones that helps the growth of cancerous cells.

- Biologic Therapy

Biologic therapy is a treatment option that involves the use of living organisms, substances derived from living organisms, or laboratory-produced versions of living organisms. It is is an innovative option and still under investigation for prostate cancer

- Bisphosphonate Therapy

Bisphosphonates are a relatively newer class of drugs which have been used for the prevention of skeletal-related complications of age-related osteoporosis or metastatic disease from carcinoma breast or multiple myeloma. Their role in the management of prostate cancer is still under evolution.

2.2 PROSTATE BIOPSY

PBx is a procedure whose aim is to investigate the presence of cancerous cells inside the prostate after an abnormal result in a screening test. To achieve it, a hollow needle is used to take a number of samples of tissue of the patient prostate under image guidance. A spring-loaded mechanism (biopsy gun), controlled by the surgeon, cause a fast extension and retraction of the needle final portion so that a small cylinder of tissue (core) is retained inside the needle (Figure 3 shows the classical set-up for the biopsy). The access to the prostate can be done through the rectum (transrectal PBx) or through the perineum (transperineal PBx).

The number of samples and the criterion with which the samples are taken can vary; the objective is to have a balance between high accuracy in one hand, and in the other the minimization of discomfort and risks for the patient.

All the possible alternatives, with advantages and disadvantages, will be discussed in this chapter.
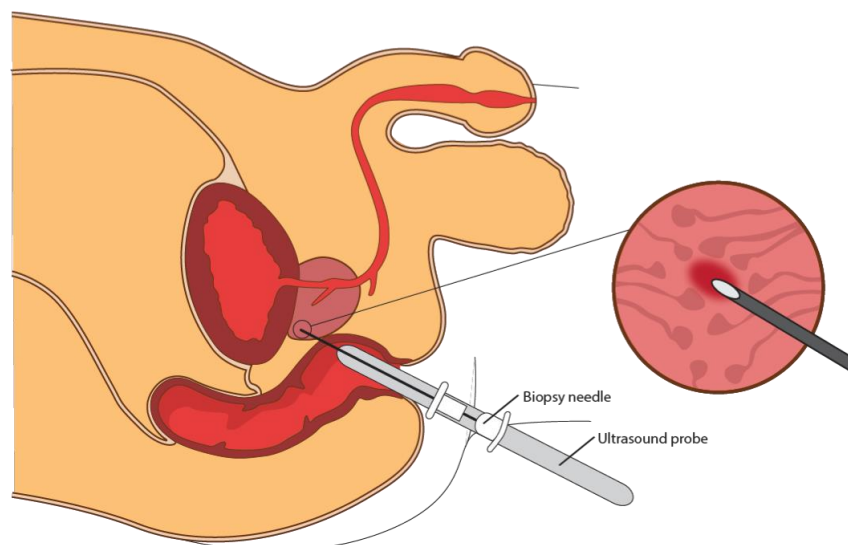
Figure 3: End-Firing TRUS
The image shows how the transrectal TRUS-guided prostate biopsy is executed; an ultrasound probe and a biopsy needle are inserted in the rectum, and the needle pierces through the rectal wall in order to access the prostate tissue and take a sample. The instrument used in this example is an end-firing TRUS that integrates the biopsy needle and the US probe in on instrument.
(*Image courtesy of Katja Tetzlaff*)

2.2.1 SAMPLES

The analysis of prostate samples under the microscope is the most accurate way to determine weather cancerous cells are present. PBx is usually executed after other screening test that include images, for this reason the ideal procedure would be taking samples only from the suspicious areas reducing the risks and discomfort for the patient, and to maximize the accuracy. However, the most used protocols for PBx makes the prostate the only solid organ in which a blind method is preferred to a targeted image-guided method[24].

Systematic biopsy methods

In the systematic methods for PBx a fixed number of samples is taken randomly from different areas of the prostate; currently, this is the most spread method for PBx, and in most of the cases this is enough to evaluate the status of the patient[25]. There are two main reasons why this approach is used: the first one is because usually the biopsy is performed under the guidance of TRUS that does not give any information about the location of all the

suspicious lesions, and the second is that in some case there is no way to detect the lesion even in mp-MRI.

There is an ongoing debate regarding the optimal number of samples that has to be taken, and the performances of different approaches have been tested. Different studies have shown discording results in term of which method performs better since the results are dependent on the group of patient, what has been found is that increasing the number of samples does not necessary leads to a higher detection rate, while it can increase the risk of complications. The number has to be chosen in order to minimize the number of false positive avoiding an oversampling, and should be chosen depending on the prostate dimension and PSA level. Some of the standard protocols are the following[26]:

- Sextant biopsy protocol (6 cores)

It has been proposed in 1989, and it is the standard reference method for PBx. This method is still used even if it has been shown that this protocol missed between 10% and 30% of the cancers[26][27].

- Extended lateral PZ biopsy protocol (10-12 cores)

This protocol extends the sextant biopsy protocol increasing the PZ sampling by adding for or six lateral cores to the standard protocol. As it as been said the results in term of accuracy depends on the study group, but the overall result has been an improvement in detection rate over the sextant biopsy protocol[27][28]. Currently, this protocol is usually the preferred one.

- Extended lateral PZ and TZ biopsy protocol (14-16-18 cores)

This protocol extends the lateral PZ biopsy protocol by adding biopsies in the TZ. It can be both an extension of the 10 cores or 12 cores, and the biopsies in the TZ can be 2 or 3 taken from each side of the TZ[28][29].

- Extended lateral PZ, TZ and midline PZ biopsy protocol (21-core)

This protocol extends the 12 cores protocol by adding 3 biopsies in the midline PZ[29].

Figure 4 shows the spatial distribution of the cores for some of the described protocols.
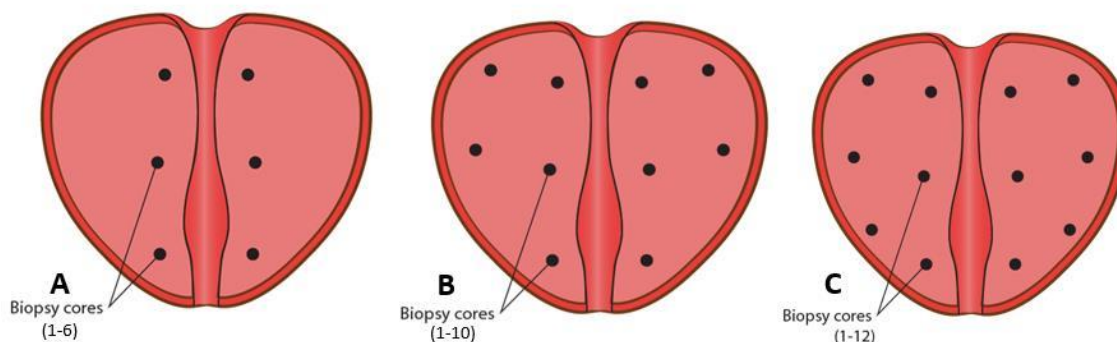
Figure 4: Templates for Systematic Prostate Biopsy
A) 6-core biopsy template B) 10-core biopsy template C) 12-core biopsy template.
(*Image courtesy of Katja Tetzlaff*)

Stereotactic transperineal prostate biopsy (STPB)

The STPB is an approach for executing a guided systematic sampling of the prostate. This method is usually used as secondary detection technique when previous biopsy shows a negative result. The STPB is performed taking about 40 samples through transperineal tissue using a template to guide the needle in the different regions of the prostate[30]. This method has shown good results not only for detecting occult carcinomas in the prostate, but also for their localization in order to perform an accurate therapy[31].

Targeted biopsy methods

Despite systematic biopsy methods are still the most used; the advent of new image technologies has increased the number of visible cancer increasing the opportunity of developing protocols for targeted biopsy with several benefits over systematic PBx. The hope is that targeted biopsy can reduce the number of false negative avoiding an oversampling during PBx procedure. The guidance to achieve a targeted biopsy can be provided whether by US images or by using MRI-US image fusion[24][25]. The possible techniques using US and enhanced US images are listed in the following list, while a more specific description of MRI-US image fusion techniques is given in section 2.2.2:

- Targeting of hypoechoic nodules

The hypoechoic nodules are those suspicious lesions that cause an increase of vessel density visible in US images. Some studies have shown that targeting those visible

abnormalities, instead of proceeding with a systematic biopsy, can increase the sensitivity of PBx but with a low specificity[25].

- PDU –Targeted biopsy

The PDU is a method of Doppler imaging that uses the amplitude of the signal instead of the frequency shift, with the advantage of the visualization of vessels with slower flow[32]. Those images can identify suspicious lesions and has been used in protocols for targeted PBx. This technique has shown to have a better diagnostic performance then the targeting of hypoechoic nodules with standard US images[25][33].

- Contrast enhanced Doppler-targeted biopsy

Color Doppler images can be also acquired after the injection of a contrast agent. The enhanced images have been used for targeted-biopsy showing an improvement in diagnostic efficiency for the PZ of the prostate[25][34].

2.2.2 MRI-GUIDED PROSTATE BIOPSY

The improvement of mp-MRI with an increasing capability in discrimination has led to the development of targeted biopsy technique whose guidance includes information provided by MRI. The main idea is to target the lesions detected by MRI while real time images of the needle are obtained through TRUS[24][35].

The available techniques that use MRI for guidance of PBx can be divided in three groups[4]:

- Cognitive Fusion

The cognitive fusion is the simplest method to us the information of MRI while performing the PBx. The physician performs the biopsy with the conventional TRUS and without the need of special equipment, but using the knowledge acquired by MRI to choose the area in which perform the biopsy[24]. From different studies, it appears that this method may improve the detection of tumor over the systematic method, but the performance is strongly dependent on the physician cognitive capability of integrating the information from MRI and TRUS[36].

- Direct MRI-guided biopsy

The direct MRI-guided biopsy is performed using an open MRI scanner or with the patient inside a closed MRI scanner[37]. For each biopsy sample and MRI image is acquired and compared with a MRI performed beforehand showing the lesion, the images are then used to evaluate the localization of the needle respect to the target. The advantage of this method is that the number of samples is limited to the target regions, but the disadvantage is that it requires a long time and expense[35][4].

- MRI-TRUS image fusion

For this method, a 3D model of the prostate is reconstructed from MRI and fused with the images obtained from TRUS; in this way the MRI provides the information regarding the cancer position, and this information is fused with the real-time images provided by the TRUS. The physician is supported with an augmented information that allows a fast and targeted biopsy, but it requires additional devices, training and an accurate fusion technology[4].

2.2.3 BIOPSY ACCESS POINT

The position of the prostate allows two different access points as shown in Figure 5. The first approach consists in the use of a transrectal needle, the needle reaches the prostate by piercing through the rectal wall. This method is the conventional one, it requires prophylactic antibiotics to avoid sepsis and it grants an easy access to the posterior part of the prostate. The second approach is the transperineal biopsy that is performed under local anesthesia with the needle piercing the perineum to reach the prostate gland parallel to the urethra. In term of patient safety, the transperineal approach reduces the risk of infection avoiding any contact with the bacteria present in the rectum, while the anatomical advantages of the second approach are an improved sampling of prostate anterior and apical region, together with a reduced risk of damage to the urethra. However, the use of the transperineal approach is limited by the need of anesthesia, an increased time and higher cost, for those reasons nowadays the transperineal approach has a major role as a secondary investigation method for those patient with previous negative transrectal biopsy[38][39].
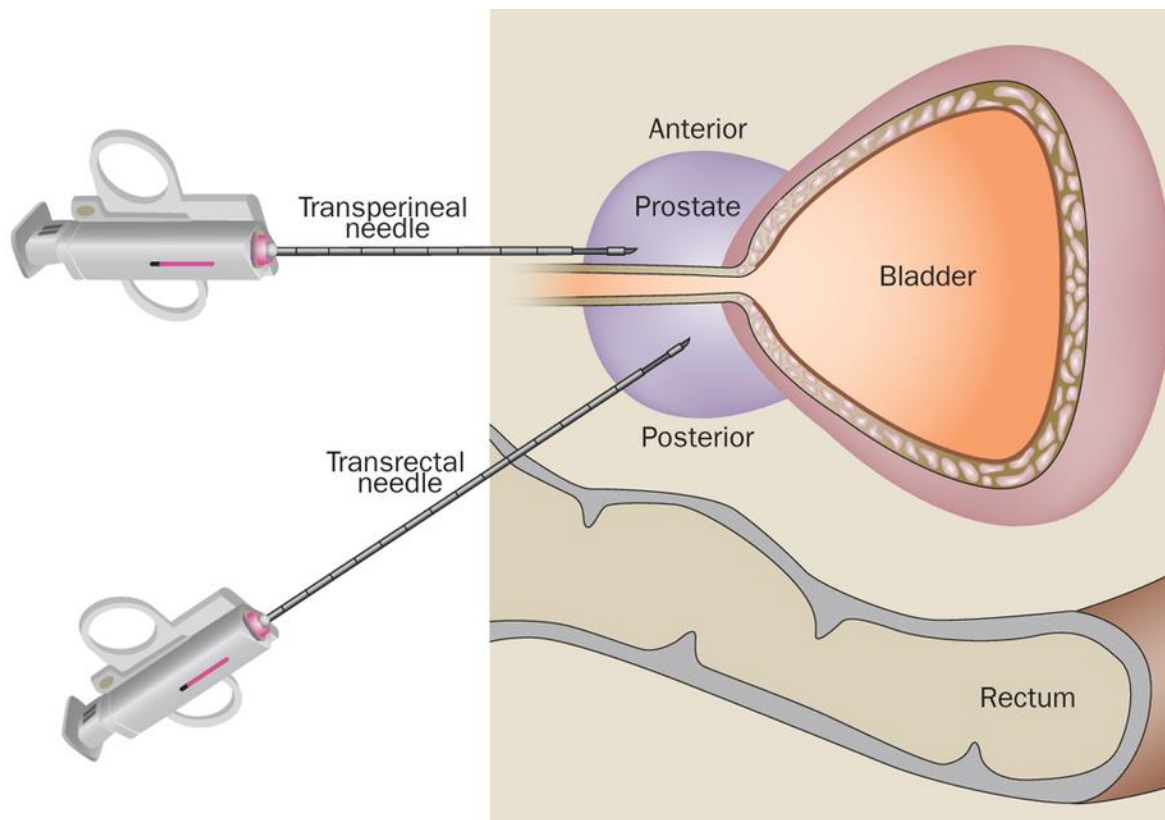
Figure 5: Comparison of Transperineal and Transrectal Approaches
In the transrectal approach the access to the gland is gained through the rectal wall, in the transperineal approach instead the needle pierces through the perineum to reach the prostate.
(Reprinted with permission from "*Transperineal biopsy of the prostate-is this the future?*"[38])

Different studies have provided discording results in term of detection rate of transrectal and transperineal approach. When a systematic biopsy is executed, the results show sometimes no statistical differences between the two methods, and sometimes an improved detection rate using the transperineal approach[40][41]. The interesting thing is that, when the biopsy is MRI-guided, the transperineal approach shows a significantly higher detection rate and it is often preferred to the transrectal approach[38].

2.2.4 PAIN AND COMPLICATIONS

The evaluation of the different biopsy technique should not be based only on the results in term of accuracy and specificity, but it should also take into consideration the discomfort of the patient during the procedure, the pain, and the risk of complications.

The PBx is a painful procedure, even if this aspect is largely ignored in clinical practice. The pain during the procedure is due to two main factors: the insertion of the ultrasound probe that causes the mechanical stretching of anal sphincter, and the puncture of the thick (16 – 18 gauge) biopsy needle. The pain is associated with the duration of the procedure and the number of cores, the way to reduce this pain is to use local anesthesia which can be done through periprostatic nerve block[42].

Even if it is considered a safe procedure, a PBx can lead to the occurrence of complications. The risk is the occurrence of infections in the urinary tract, sepsis and prostatitis. The number of infections has increased in the last 20 years due to the increase of antibiotic resistant bacteria, while the number of noninfectious complication has remained constant[43][44].

2.3 SURGICAL NAVIGATION SYSTEMS

Surgical Navigation systems is a broad term, it is the ensemble of all the technologies providing surgeon with the information regarding the anatomical position of the instrument, the location of the target and the safest way to reach the target. Those technologies have spread in the last two decades thanks to the improvements in image techniques and the growth of computer processing capabilities. Those systems result in safer and less invasive surgical procedures[5].

The principles for surgery navigation systems are presented in this section, together with one example from the literature similar to the one proposed in this project.

2.3.1 PRINCIPLES OF SURGICAL NAVIGATION SYSTEMS

Surgical navigation system is a localization technology able to compute the position of surgical instruments and anatomical target in a global coordinate system, and to provide the surgeon with this information, in order to enhance the knowledge of the environment and increase the confidence.

A variety of navigation systems are now available, platforms have been developed in order to comply with the requirements of different surgical tasks[5]. The common steps are:

- Modeling/Image acquisition

The system requires information regarding the anatomy of the patient and the position of the targets inside the anatomy. This is usually achieved thanks to the acquisition medical images and/or the definition of a virtual model.

- Instrument Tracking

The position and orientation of the instrument is tracked in 3D space, the two methods that are generally used for the tracking of the devices are optical and electromagnetic tracking systems[45].

- Registration

The measure of the instrument position and the models are obtained in different coordinate systems, the relation between them is computed via the registration process. Usually, in order to successfully accomplish this step some "fiducial points" are placed on the patient, those points are measured in both the coordinates and they are used to compute the transform between one system and the other.

- Processing

The registration process provide the matched models of instrumentation and anatomy, and in some case it is followed by a further processing to obtain all the information required by the surgeon for the navigation.

- Display

The last step is the presentation of the information at the surgeon. In most of the case this is done visually trough 2D or 3D images, but any kind of stimuli can be used depending on the application (for example an haptical feedback can be preferred).

Surgical Navigation System
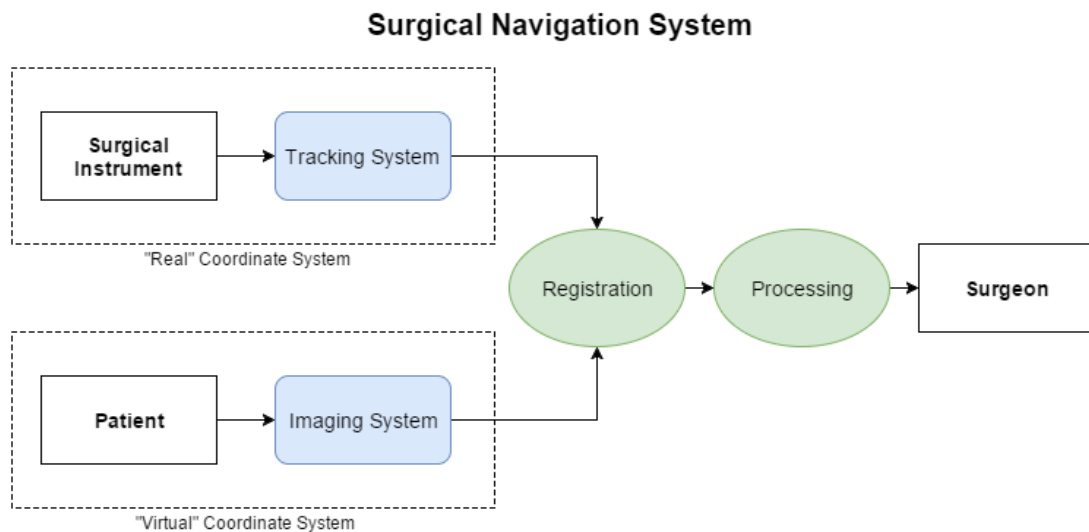
Figure 6: General Scheme of a Surgical Navigation Systems
A surgical navigation system register the images of the patient to the position of the devices, process those information, and gives the surgeon a feedback on the status of the surgical environment.

2.3.2 EXAMPLE: FRAME-LESS STEREOTAXY FOR BRAIN BIOPSY

Neurosurgery is the surgical field in which surgical navigation systems have found higher application, the reason is that brain surgery needs to be as minimally invasive and precise as possible[5]. In this field, the frame-less stereotaxy biopsy is an example of implementation of a surgical navigation system based on real-time virtual reality feedback[46].

Even if today the frame-based stereotaxy remains the standard procedure, frame-less set up has comparable accuracy, but it involves a reduction in time and in the number of complications[47].

The stereotaxy is a procedure for the targeting of structures inside the brain with a minimally invasive approach. In the frame-based stereotaxy, in order to achieve this targeting, a physical mechanical frame is attached to the patient. The frame is an arc-quadrant system that allows the targeting of a 3D location inside the brain.

In the frame-less stereotaxy system the frame is replaced by a navigation system based on virtual images and instrument tracking. The MRI of the patient is examined in the pre-

operative phase, and both the target position and the needle trajectory are determined. Then the images are registered to the patient position through fiducial markers or using surface merging algorithms. The main challenge in achieving the registration is the fact that tissues are deformable, and deformations occur between pre-operative intra-operative images; for this reason, often complex algorithms for non-rigid registration are required. Merging those information those information the surgeon is offered a navigation system that tracks in real time the position of the needle merging this information with the pre-operative images[48]. Furthermore, all those information can be shared also with a Computer-Aided system for the control of the positioning of the needle in order to achieve higher level of accuracy[46].
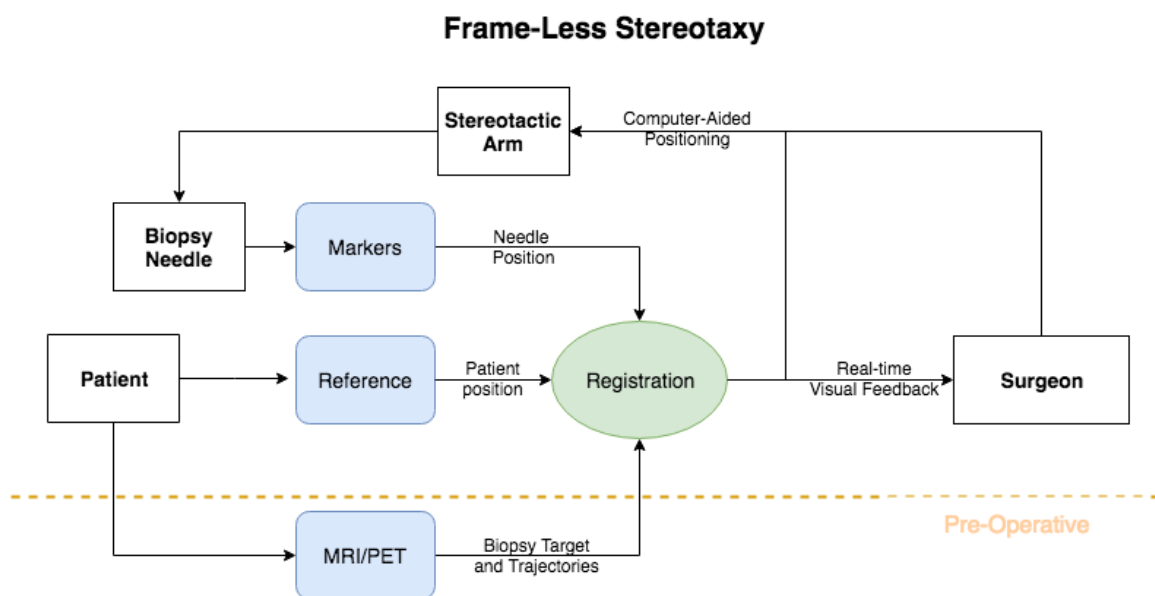
Figure 7: Scheme of Frame-Less Stereotaxy Navigation
In the proposed frame-less stereotaxy navigation system, a reference system is attached to the patient in order to register the position of the needle to the pre-operative images. The information is fused to give the surgeon a real-time visual feedback and to control the stereotactic arm for the positioning of the needle.

3 APPROACH[1]

3.1 MOTIVATION

The section 2.2 presents the available techniques for PBx navigation discussing advantages and disadvantages of each technique. It is noticeable that in the last decades many attempts have been made in order to take advantage of modern technologies to move from blind TRUS-guided biopsy to targeted MRI-guided biopsy. However, even if TRUS-MRI fusion guidance has proved to be an alternative to the standard systematic biopsy, the high complexity and cost of those systems is not justified by improved performances.

In this section, it is motivated the need of a new approach for PBx navigation system to overtake the weakness of the available systems.

3.1.1 TARGETED BIOPSY (REAL-TIME TRACKING)

The standard methods for PBx use the TRUS alone as guidance during the navigation, with the problem that US images do not give any information about location of suspicious area. The use of the TRUS has led to the development of systematic blind biopsy techniques, those techniques are based on the assumption that with a sufficient sampling rate it is possible to determine whether cancerous cells are present or not. Even if this approach has proved to be

---

[1] This chapter has been partially taken from the works of the author at [66][67]

clinically valid, it neglects the information that modern MRI techniques can provide about presence and location of cancerous cells (as described in section 2.1); if used to target the suspicious areas, this information can improve the detection rate and prevent risks and complications due to oversampling of the prostate.

The techniques of MRI-TRUS fusion introduced in the last few years are described in section 2.2, the information provided by TRUS is integrated with the MRI in order to achieve a targeted biopsy. The fusion techniques are implemented through the segmentation of prostate MRI, an algorithm of automatic segmentation of the US images, and an algorithm that matches the two images. In many case, compared to the standard systematic biopsy, the fusion biopsy has shown an improved detection rate and shorter surgical time[49]; however, this approach has significant higher costs, complexity and total time (which includes the image segmentation and the setting of the system) that affects both the surgeon mental load and the hospital balance. What makes this approach computationally costly are the elastic properties of prostate and surrounding tissues. The configuration of the prostate during the procedure and during the MRI scanning is different, the image fusion software has to be accurate and efficient in order to compute in real-time the deformation that maps the MRI volume in the US image. Only in this way the position of the target can be tracked and displayed to the surgeon.

While the inclusion of MRI to perform targeted biopsy represent an improvement over the systematic methods, the image fusion is a complex and inefficient process; for this reason, the aim of the project is to develop a navigation system that uses MRI to target suspicious areas, avoiding the TRUS-MRI fusion.

3.1.2 TRUS

The TRUS has always been the principal instrument for the navigation during the PBx procedure since it can provide real-time images of the needle inside the pelvis. As explained in chapter 2, the weakness of TRUS images is that most of the cancerous tissues are isoechoic, which means that the detection capability of US images in practice is null. Moreover, the TRUS is a cause of discomfort and pain for the patient. Nevertheless, the

TRUS remains a key element for the navigation even when MRI guided targeted biopsy is performed.

The main problem of TRUS-MRI fusion, cited in the previous section (3.1.1), is the matching of the real-time images of the deformed prostate and the pre-operative MRI. The TRUS plays an important role in this deformation; the US probe is pushed through the rectum in proximity of the prostate causing a major deformation of the tissues that increasing the mismatch between pre-operative MRI and real-time TRUS images.

The role of the TRUS in TRUS-MRI fusion biopsy can be summarized in two main functions: real-time tracking of the instrument and real-time tracking of the tissue deformation in case of TRUS-MRI fusion. Since the presence of the TRUS itself is one of the reasons why the tissue deforms, it is reasonable to think at alternative real-time tracking technologies.

3.2 PROPOSED SOLUTION

Given the problems discussed above, the proposed solution is a *virtual reality navigation system for targeted biopsy* in which a transperineal targeted biopsy is executed under the guidance of virtual images. The 3D virtual images are obtained combining pre-operative MRI of the patient with a virtual needle tracked with an EMTS.

Before the procedure the patient is scanned to obtain a volumetric image (MRI, that can be combined with other image techniques) and the tracking system is registered to the anatomical data through fiducial markers registration. During the procedure, the position of the needle is tracked by a sensor, while a sensor corrects the registration accordingly to patient pelvis displacements. Information are combined in a graphical interface that provide the surgeon visual feedback of the needle position respect to the internal anatomy.

An overview of the system workflow, as shown in Figure 8, is presented in this section. In the following chapter (chapter 4) the way in which it has been implemented will be explained.
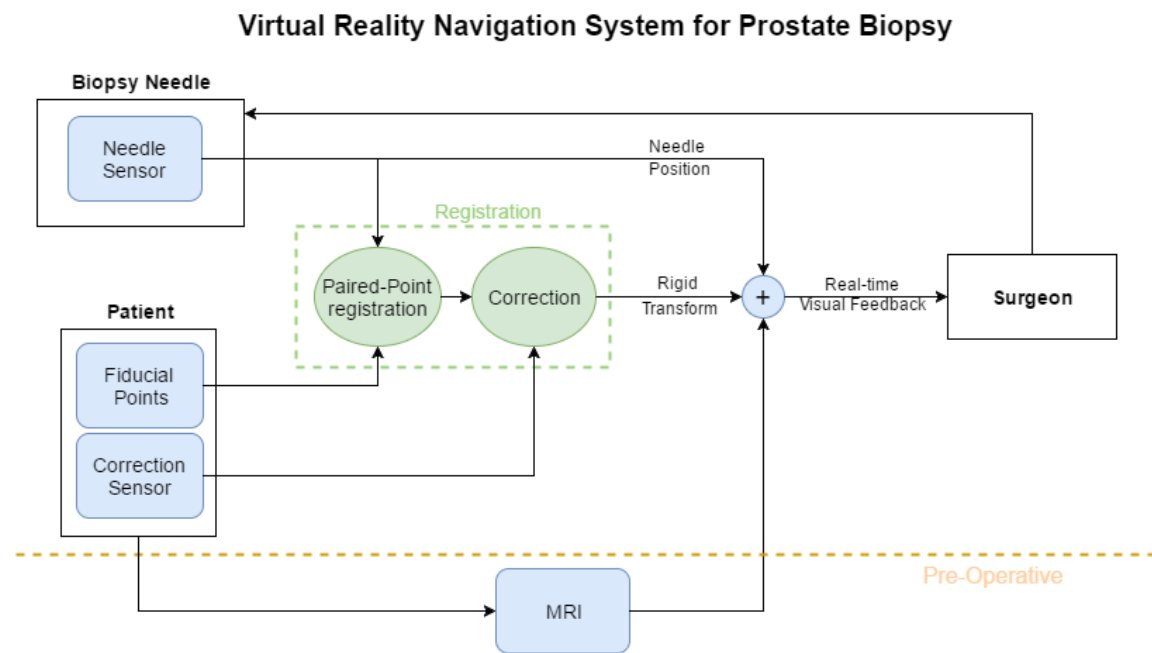
Figure 8: Scheme of the Virtual Reality Navigation System for Prostate Biopsy
In the proposed navigation system, a rigid transform register the position of the needle to the patient MRI.
The transform is obtained in two steps: a paired-point registration of the position of fiducial markers
(fiducial points), and a real-time correction through a sensor placed on the patient pelvis. The surgeon is
offered a real-time visual feedback of the position of the needle in the MRI volume.

3.2.1 PRE-OPERATIVE IMAGING

The first step of the system is the acquisition of the model that will be the anatomical
reference during the navigation, the model is obtained from pre-operative volumetric
imaging of the pelvis. To avoid changes in patient anatomy between the image acquisition
and the procedure, the patient should be scanned as close as possible to the procedure
execution.

The volume can be a simple mp-MRI loaded as it is after the acquisition or it can be the
outcome of image processing in order to enhance and fuse the information from different
image techniques. The system can also load and display 3D meshes segmented from the
images. The idea is to have a flexible system able to use MRI images without requiring pre-
processing, but that can also incorporate additional information whether required or
available.

During the image acquisition, some visible markers are placed on the pelvis skin; those markers remain on the patient until the biopsy is performed in order to register the anatomical model to the instrument tracking system. Before moving to the registration step, the position of the markers in the volumetric image has to be determined together with the position of the biopsy targets.

3.2.2 INSTRUMENT TRACKING

During the procedure, an EMTS is used to get 3D position and orientation of the needle in the surgical field replacing the TRUS as instrument for real-time tracking. The measurements are done using an electromagnetic sensor placed on the instrument (the *needle sensor)* and are relative to an electro-magnetic transmitter. In order to combine this information with the volume images, the relationship between the tracker coordinate system and the pelvis model has to be determined.

The use of EMTS overtakes the problem of the TRUS discussed in the previous section (3.1); moreover, if with the TRUS the position of the needle is derived from the surrounding visible tissues and this can be done only when the needle is in the visual field of the US, with the EMTS the position of the needle is always known once the registration is done. As consequence, the *virtual reality navigation system for prostate biopsy* not only offers guidance when the needle is inside the patient, but also guides the urology during the access through the perineum (replacing the STPB).

3.2.3 REGISTRATION AND CORRECTION

The last step, before the biopsy is performed, is to map in real-time the coordinates of the needle to the patient anatomy model accordingly to the patient position. This process, named registration process, is executed right before the biopsy procedure, with the patient in the surgical lithotomy position.

In order to obtain the transform that maps the two coordinate systems, the tracker is turned on, and the needle is used to determine the position of the markers in the EMTS coordinate

system. Since the position of the markers in the virtual coordinate system is known, a paired-point registration algorithm matches the two coordinate systems determining the transform matrix.

The paired point registration is a static process completed before the procedure and it does not take into account the intra-operative rigid displacements of the prostate. For this reason a second sensor, the *correction sensor,* is placed on the patient pelvis to preserve the matching between the two systems updating the registration transform.

3.2.4 VISUAL FEEDBACK

During the procedure, a visual feedback is provided to the surgeon through a 3D monitor. The graphic interface displays virtual images of needle and internal anatomy both in a 3D environment and in three 2D orthogonal projection of the volume.

Furthermore, the information displayed is enhanced with some extra features for guided navigation and targeted biopsy. Those features include the position of the core previously taken, the distance between the needle and the target, the shot range of the needle and the direction from the needle tip to the target point.

The information should allow the surgeon to perform efficiently a targeted biopsy without an overload of information. For this reason, it is important that the graphical interface is intuitive and flexible to adapt to patient condition and surgeon preferences.

3.2.5 PROBLEMS

The biggest problem with this approach concerns the overall accuracy of the system in the registration. Accordingly to literature, the required target registration error for targeting small lesions is <1.9mm[50].

The first main source of error is the non-rigid properties of the prostate tissue, while the proposed approach uses a rigid transform to do the registration and track the prostate displacements.

The second problem concerns the displacement of the prostate respect to the reference sensor that is positioned on the pelvis, and their position is not strictly correlated since the prostate can move respect to the perineum tissue,

For this reason those aspects still need to be evaluated and tested, the idea is that even if a targeting registration error <1,9 mm can not be achieved, the system could be an instrument to target larger suspicious areas (e.g. >1ml).

4 MATERIALS AND METHODS[1]

4.1 LACE (SOFTWARE)

The *LACE Library* is a C++ middleware platform for virtual reality (VR) and augmented reality (AR) applications; it has been developed in order to overcome the lack of internal communication between the software-hardware environments needed for this project, and for three other projects developed in the Mixed Reality Lab of the UIC[51][52][53].

LACE Library has been developed as the integration of different software-hardware environments, as shown in Figure 9. The tasks achieved by *LACE* are:

- Graphics Rendering

It is based on Visualization Library[54] (VL), an OpenGL[55] based Open Source library, for 2D and 3D graphics application, that maintains the flexibility and high performances of OpenGL with intuitive and user-friendly structure of classes and functions.

- 3D Tracking

The library works both with the Ascension 3D Guidance® system[56] (AS), and with the tracking systems by Northern Digital Incorporated[57] (NDI). The Ascension system is an EMTS that communicates through the C++ 3D Guidance API. For the communication with NDI instrumentation, the communication is done through the open

---

[1] This chapter has been partially taken from the works of the author at [66][67]

source library NDI Combined API[58] that works with Aurora (EMTS) and Polaris (Optical Tracking System).

- Haptics Rendering

It is based on QuickHaptics[TM][59] (QH), a software development toolkit provided for the communication with the haptic devices of 3D Systems Geomagic®, and built upon 3D Systems OpenHaptics®. QH allows to create haptical rendered objects and to define custom haptic effects.

- Wykobi Computational Geometry Library[60] (VL)

2D and 3D computational geometry library.

The graphical rendering, the haptical rendering and the 3D tracking have been organized in a structure that create and optimizes communication between the different components. The graphics rendering and the 3D tracking happen synchronously at the rendering frequency (60Hz unless specified otherwise), meanwhile the haptics rendering runs on a different thread at 1KHz.

LACE is organized in such a way that VL handles the entire graphic rendering of the scene using the information from the hardware components (haptic device, electromagnetic tracker and standard input/output hardware), and shares the information with QH for the haptical rendering of objects and forces. The OpenGL high graphic performances are fully integrated in *LACE* through VL, the developer has many different options in terms of visualization and it is offered an easy user-friendly interface for advanced rendering techniques (such as stereoscopic view and volume ray casting).

The library, implemented and tested for VR medical applications, has result is a general-purpose platform for the development of VR/AR software. In this section, it is presented an overview of the library structure and implementation.
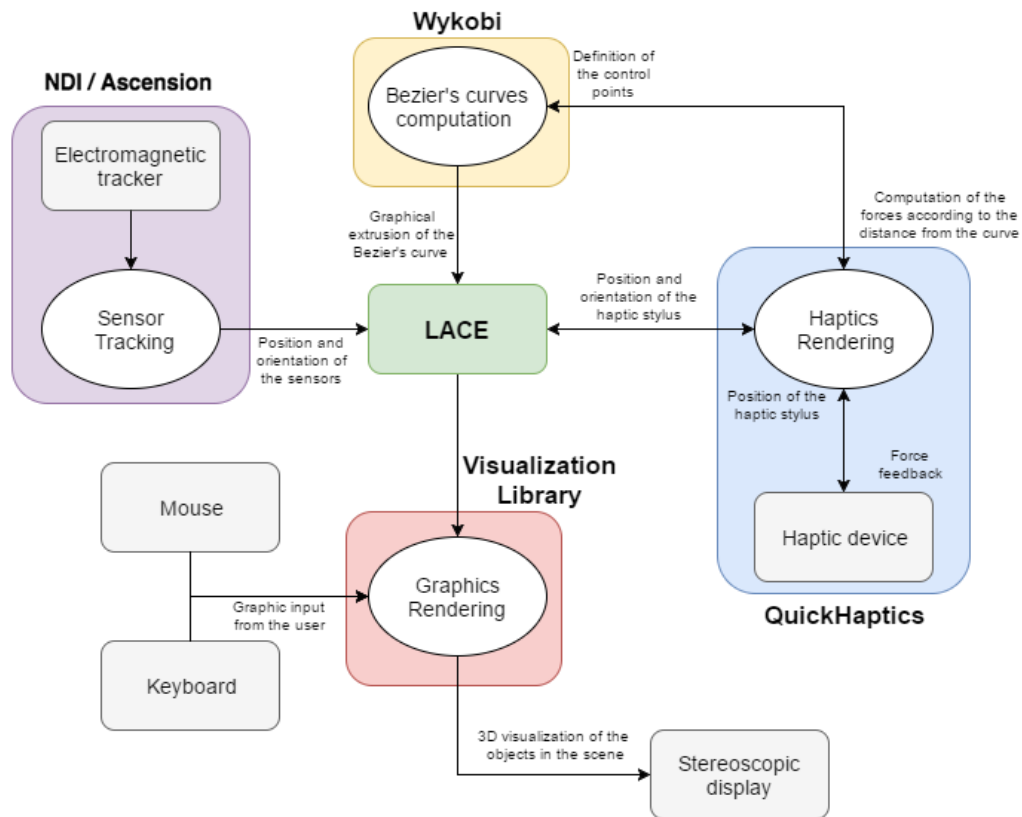
Figure 9: LACE Library Communication Workflow
Workflow of the communication between *LACE Library* and hardware components. The four library components of *LACE* communicate with the hardware and with *LACE*. The *LACE Library*, in the middle, gets the data from QuickHaptics[TM], Wykobi and Ascension/NDI API, and passes the data to Visualization Library for the visual rendering and to QuickHaptics[TM] for the rendering of forces.

4.1.1 CLASSES

The communication between the four libraries is achieved through *LACE library* class structure. The *LACE* classes interface the component libraries and communicate internally sharing information; Figure 10 shows the general flow of the internal communication between *LACE* classes, and how they interface the four libraries.
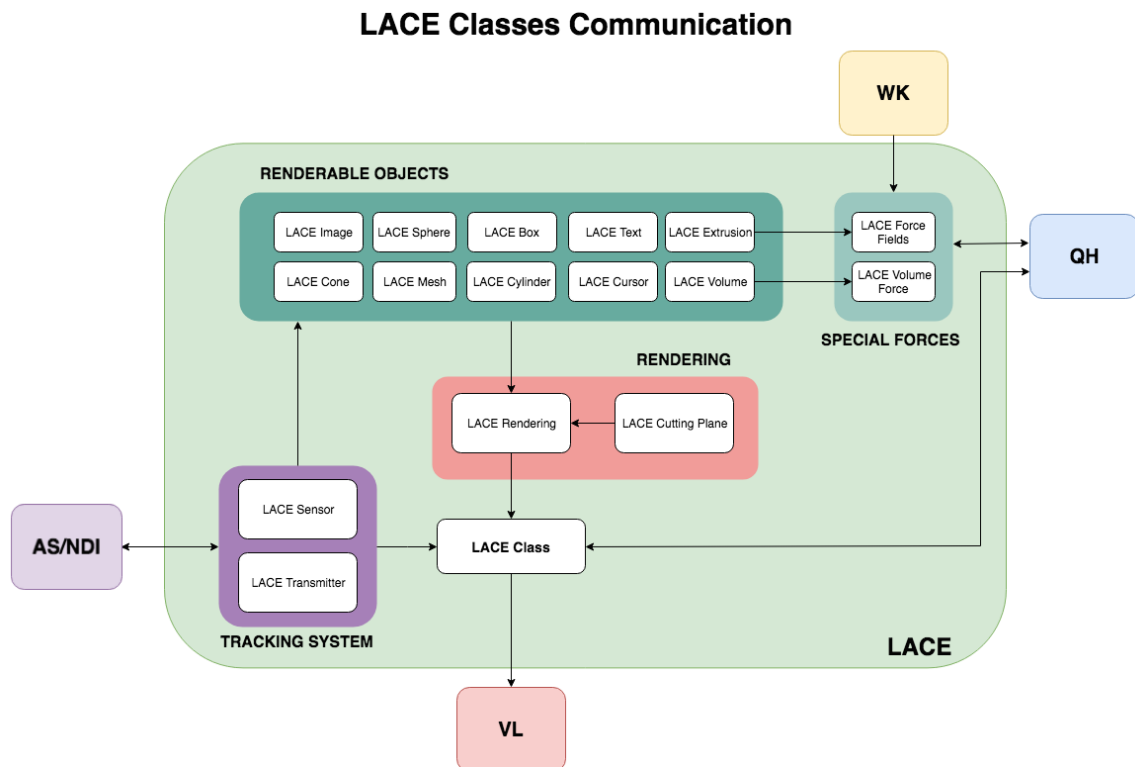
Figure 10: LACE Classes internal/external communication
Workflow of the internal communication between *LACE* classes, and of the interfaces with the library components. *LACE Class* is the central component of the library, it gets data from renderable objects, sensors, renderings and devices. The *LACE Class* communicates directly with QuickHaptics™ devices and with Ascension through the *LACE Sensor* and *LACE Transmitter* classes. In some case, some special forces are computed using the computational capacity of Wykobi Computational Geometry Library.

To better describe the role of each class, four groups of classes can be defined:

- Renderable Objects Classes

The classes that allow the creation of haptically and graphically rendered objects compose this group. All those classes are derived from the base class *LACE Object* that implements the communication between QH and VL. The *LACE* renderable objects are: Box, Cone, Cylinder, Sphere, Volume, Mesh, Image and Extrusion.

- Tracking System Classes

This group includes the classes *LACE Transmitter* and *LACE Sensor* that communicates with AS.

- Special Forces Classes

LACE Volume Force and *LACE Force Field* are the two classes composing this group. Those classes can be associated respectively to a *LACE Volume* and a *LACE Extrusion* in order to render special force fields.

- Rendering Classes

LACE Library allows the creation of multiple rendering in the scene, each rendering is defined as a *LACE Rendering* class instance. *LACE Rendering* contains both a list of the objects to be rendered and all the rendering parameters (parameters of camera and viewport). In this group it can also be included the class *LACE Cutting Plane* that implements the possibility to cut one or more *LACE Object*.

At the top of those classes there is the class *LACE Class* that contains pointers to all the elements of the application and handles their creation, initialization and update. The *LACE Class* is a singleton class that is always created in every *LACE* application.

4.1.2 RENDERABLE OBJECT CLASSES

In *LACE* all the graphically and haptically renderable object inherit from the *LACE Object* base class which contains both the graphical and the haptical component of the object. *LACE Object* is the class responsible for the dynamic communication between VL and QH, Figure 11 shows how the two libraries communicates. For the graphical rendering, each *LACE Object* contains a geometry, a transform and an effect; those three elements constitute the *VL Actor*, which is the renderable object used by VL. Each *LACE Object* contains also the corresponding *QH Object* that is haptically rendered in according to the shape and the material properties; those properties are defined for the QH shape using the standard QH commands.

In order to graphically render a *LACE Object*, it is stored in one, or more, *LACE Rendering*; in this way the objects will be rendered in the OpenGL context as the *LACE* application starts.
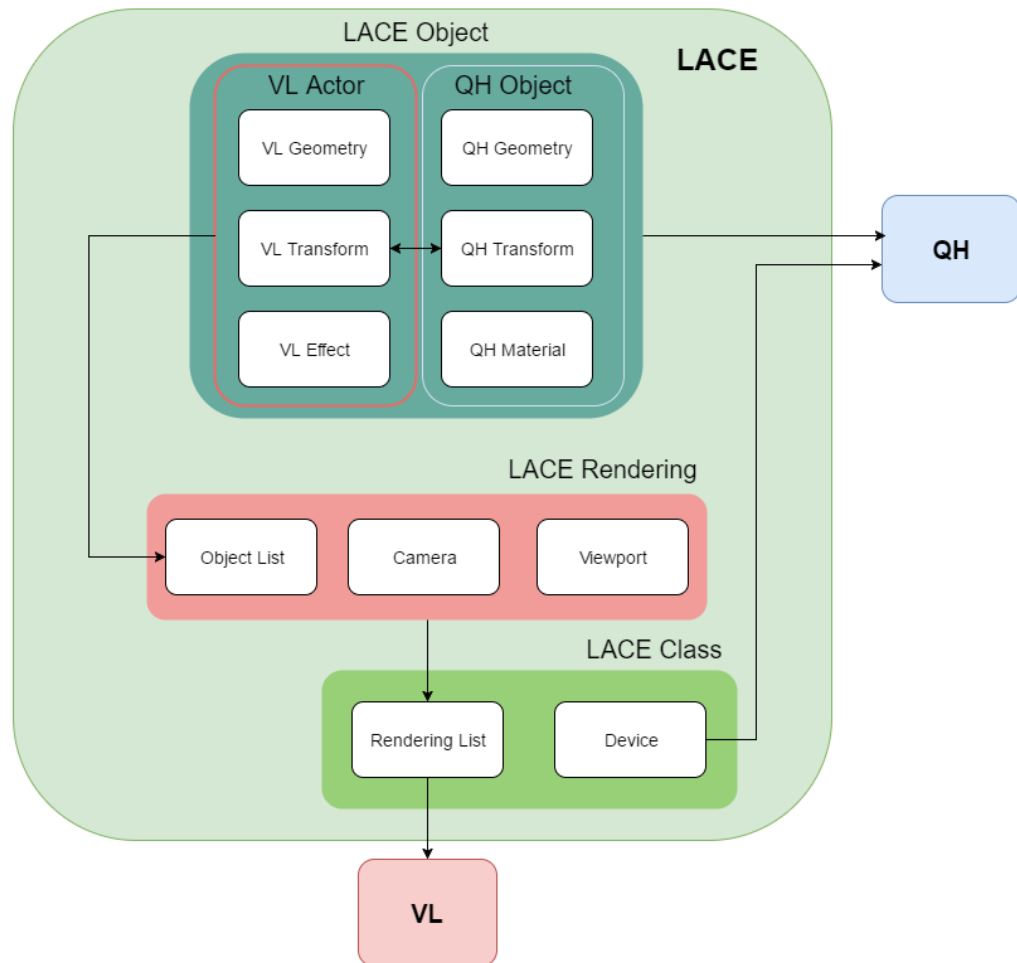
Figure 11: LACE Object Rendering
Workflow of the visual and haptical rendering of *LACE Object*. Each *LACE Object* contains a *VL Actor* and a *QH Object* that stores respectively the visual and haptical properties for the object. The haptical properties are communicated directly to the QH environment. Since *LACE* can implement multiple rendering, the graphic rendering of the object is first assigned to a *LACE Rendering* that renders the object through *LACE Class*.

LACE Transform

Once a *LACE Object* is created, an update system, shown in Figure 12, has been implemented so that the *VL Actor* and the *QH Object* maintain the same position in graphic and haptic environment. Those transforms are described by 4x4 matrices that define the rotation, translation and scale of each object in VL and in QH. To make the two environments consistent the two transforms need to be always coupled with a continuous mechanism of update.

The *LACE Transform* of each *LACE Object* can be changed applying a relative transform (rotation, translation and scaling), or can be redefined entirely with a new transform matrix. When the *LACE Transform change*, it is applied first at the *VL Actor*, and then the *VL Transform* of the *VL Actor* is copied as *QH Transform* for the *QH Object*. Each object has also a *LACE Initial Transform*, which is a transform matrix that is always pre-multiplied when a new transform matrix is assigned to the object. This transform is automatically defined for *LACE Volume* and *LACE Mesh* in order to have the matching between the different loaded file formats, otherwise for the other *LACE Object* the *LACE Initial Transform* is an identity matrix unless it is defined by the programmer.

However, since the objects in *LACE* are dynamic library, a system of continuous update allows AS/NDI and QH to control object transform matrix. In case an *AS/NDI Sensor* controls the *LACE Object*, at each graphic frame the *AS/NDI Transform* (transform matrix of the LACE *Sensor*) is assigned as *LACE Transform*. The mechanism is reversed for the haptically rendered objects; since the *QH Object* and cursors can be moved in QH environment, at each graphic frame the *VL Transform* is updated accordingly to the object *QH Transform*.

LACE Object Transform update
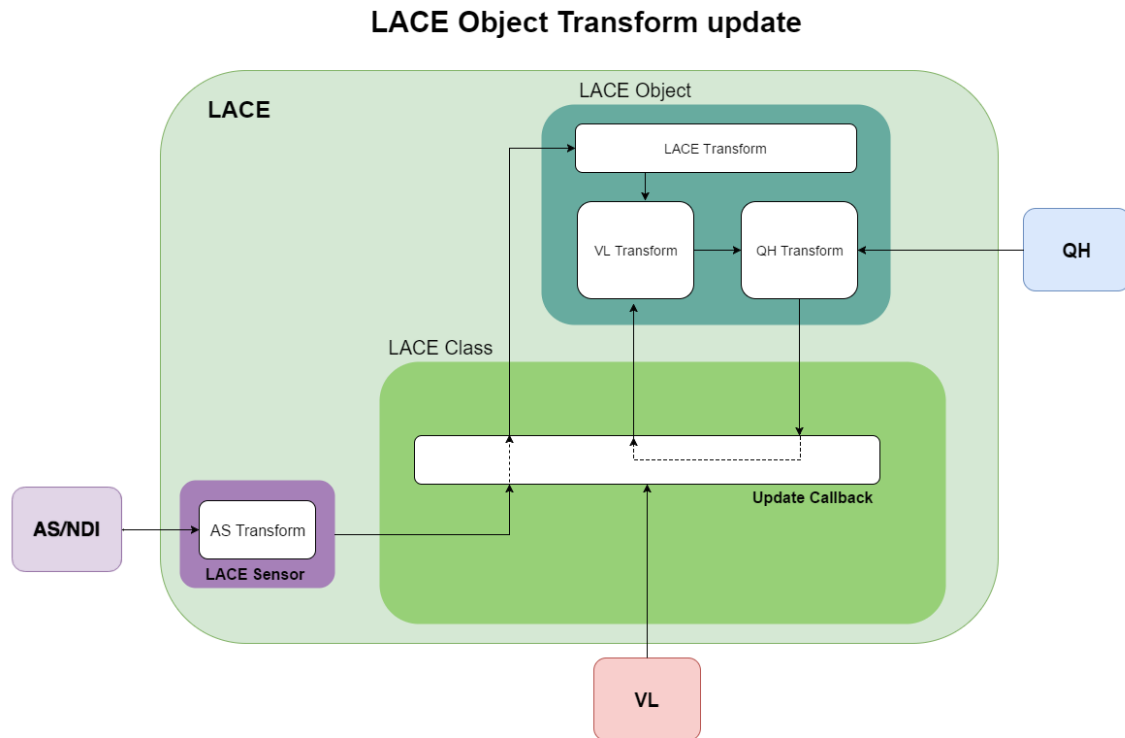
Figure 12: LACE Object Transform Update
Workflow of the object transforms synchronization in the *LACE*. When the *LACE Transform* changes, first the *VL Transform* is updated, and then the *QH Transform* is used to update the *VL Transform*. For the update of an object transform according to a sensor, the *LACE Transform* is constantly updated in the *LACE Update Callback* called by the VL thread. If QH acts on the transform of an object, the update mechanism is reversed, at the end of the LACE Update Callback the *VL Transform* is update accordingly to the *QH Transform*.

LACE Volume

LACE Volume is a *LACE Object* derived class that handles the loading and rendering of volumetric images. The volume can be loaded in different format, including DICOM and MHD files the two most common format for storing medical volume images. Three ways of volume visualization are implemented:

- volumeSLICED

The volumetric data is divided into slices that are reassembled to form a 3D image. The user can define the number of slices, the RGB transfer function, and the bias for the portion of volume that has to be displayed. This rendering modality is the only one that allows the volume clipping using *LACE Cutting Plane*.

- volumeRAYCAST

This method uses the ray cast technique to render a volume. Predefined reycasting algorithms can be used, or user-defined algorithms can be loaded. With this rendering modality, a custom-made transfer function for the R, G, B, and α channels can be tuned and controlled.

- volumeORTHOGONAL

It consists in displaying the sagittal, coronal and axial planes of the volume centered in a specific voxel. The center of the planes can be a volume coordinate, or it can be associated to the position of a *LACE Object*. The RGB transfer function used to render the planes is the same one of *volumeSLICED* rendering mode.

LACE Mesh

A polygon mesh is a set of faces, vertices and edges that sketch the shape of a polyhedral object in computer graphics. With the *LACE Mesh* class it is possible to load and render 3D shapes. If the mesh has been obtained as volume segmentation, taking into account offset and scaling factor of the volume, in *LACE* it is possible to match the mesh position and orientation with the position and orientation of the volume.

LACE Image

This class has been implemented in *LACE* to allow the loading and rendering of 2D images in the scene; those images are displayed as texture on planes. The supported formats are those supported by VL: JPG, PNG, TGA, TIFF, BMP, DDS and DICOM.

4.1.3 TRACKING SYSTEM CLASSES

The classes *LACE Transmitter* and *LACE Sensor* constitute the bridge for the communication with; Figure 13 shows the workflow of this communication.

The *LACE Transmitter* stores the system parameters and the on/off status of the transmitter that generates electromagnetic field, while the *LACE Sensor* communicates with the physical electromagnetic sensor.

Pointer to the created *LACE Transmitter* and *LACE Sensor* instances are stored in the *LACE Class* in order to have a runtime update of the status.
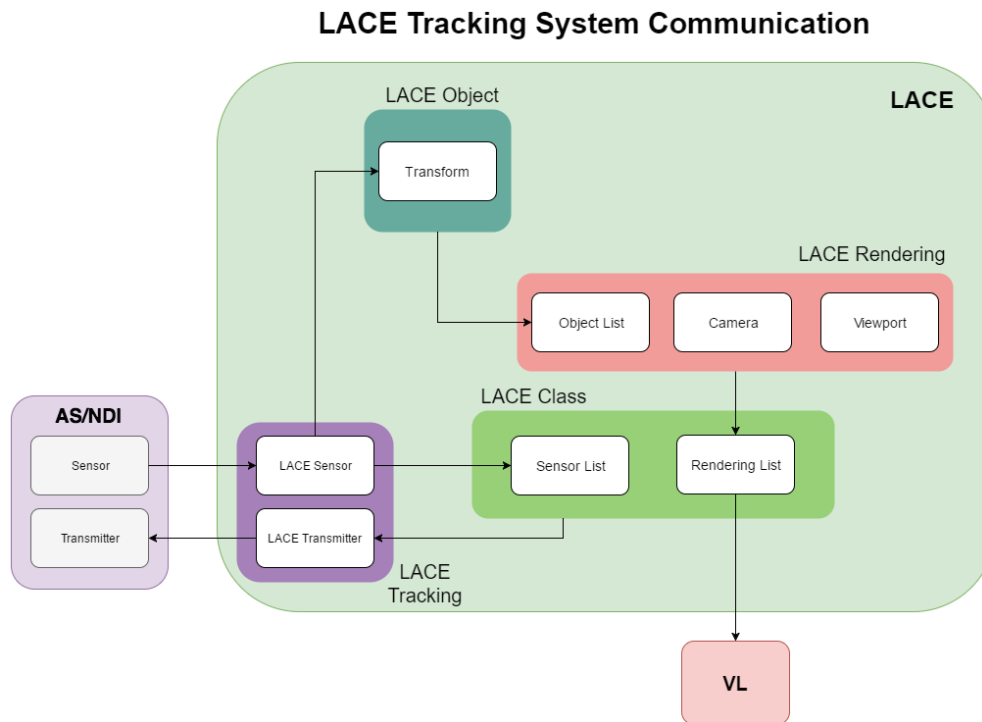
Figure 13: LACE Tracking System Communication
Workflow of the communication between *LACE* and the EMTS. The *LACE Class* controls the status of the transmitter turning it ON/OFF. The position and orientation of the sensor is communicated to a *LACE Sensor* that controls the transform of a slave *LACE Object*.

LACE Transmitter

The *LACE Transmitter* is used to control the AS/NDI transmitter and the EMTS parameters. This class implements the switch ON/OFF of the transmitter, and can be used to set unit of measure, reference system and all the other system parameters controlled by the API.

LACE Sensor

LACE Sensor is used to communicate with the physical sensor connected to the port corresponding to the *sensor ID* of *LACE Sensor*. Each *LACE Sensor* is stored in the *LACE Class* in order to synchronously update the *Transform* at each graphic frame. For a better communication with the other elements of *LACE*, the transform, read as quaternion, is converted into a 4x4 transform matrix.

It is also possible to define a *LACE Slave Object* that is constantly updated with the *sensor Transform* of the *LACE Sensor* with the mechanism shown in Figure 12.

4.1.4 LACE RENDERING

The *LACE* graphical rendering is built on the top of VL, and consequently it is based on OpenGL API. *LACE* can handle multiple renderings that displayed either in the viewport or as texture (rendering to object).

The *LACE Rendering* is the class used to define each rendering. Each *LACE Rendering* stores a list of *LACE Object* that have to be rendered. In addition, each *LACE Rendering* stores the settings of the camera, where the rendering has to be displayed (coordinates of the viewport or *LACE Object* on which apply the texture).

LACE Cutting Plane

The *LACE Cutting Plane* is a feature implemented in *LACE Library* that uses VL in order to define a cutting plane for a *LACE Object*. Once the *LACE Cutting Plane* is created, it is possible to cut as many *LACE Object* as desired using the function *Cut* of the *LACE Object class*. It is also possible to associate a *LACE Object* as master for the cutting plane so that the *LACE Object* transform controls the *LACE Cutting Plane* transform.

4.1.5 PERSONAL CONTRIBUTION

As introduced before, the *LACE library* has been developed at the UIC Mixed Reality Lab, and is the result of a collaboration of four master students, including myself, under the supervision of professor Cristian Luciano. Personally, I have been involved both in the conception of the library, and in the construction of most of the classes. Below you can find what have been the most significant contributions.

LACE Class

I have been responsible for the creation of the first instance of the *LACE Class*. In order to retain the characteristics of VL, the *LACE Class* has been created as derived class of VL *Applet Class*. In this way, it was possible to access the VL graphic callback, which is a virtual function of the *Applet Class*, and to use it for the communication with the tracker and the haptic world. In addition, it has been made possible to execute user-defined function at the callbacks (pre/post graphic callbacks, or other callbacks due to interaction with keyboard and mouse) through function pointers.

In *LACE Class* I have also created the functions that enable/disable the libraries depending on the developer request, so that only the required libraries are initialized. This functionality prevents also the running of parallel threads when not required, in this way the performances of the applications are optimized.

Moreover, I have added to *LACE library* the lists that register all the objects the application need to interact with (Renderable Objects, Sensors, Haptic Devices, Cameras). Whenever one of these objects is created, it is added to those lists through a *LACE Class* function.

Tracking System

I have been fully responsible for the integration of the tracking system in *LACE library*. I have implemented the initialization of transmitter and sensors, the reading of sensors data, the conversion of the data, and the control of scene objects through sensors. This work has been done both using the Ascension API, and the NDI Combined API.

Haptics

Even if my project doesn't involve haptics rendering, I have also worked at the integration of QuickHaptics in *LACE library*. In particular I have created the function that registers the devices in order to have the interaction with the other objects.

Multiple Renderings

I have implemented the possibility of having multiple renderings in the scene with different cameras and different objects. There is the possibility to associate each object to one, or multiple scenes, and for each of those it is possible to independently define the camera and the framebuffer (the object, or the portion of the screen where the scene has to be rendered).

This functionality was then useful for the 3D rendering definition (two different cameras and two side by side framebuffers, that render the same scene).

4.2 HARDWARE

The PBx navigation requires the use of hardware components that interact with the environment and the software. The hardware includes:

- Biopsy Needle: to perform the biopsy
- EMTS: for the tracking of the patient and the instrument.
- Monitor: for the graphic rendering.
- Fiducial point stickers: for the system registration.
- Phantom: for the system testing.

Two different set-ups have been prepared, one at the UIC, and one at the Politecnico di Milano. The specifics and the properties of the hardware components are given in this section.

4.2.1 TRACKING SYSTEM

The EMTS that has been used in Chicago is the one produced by the Ascension Technology Corporation, the specifications of the components that have been used are shown in Figure 14. In Milano, the system that has been used is the Aurora tracking system by NDI, and the specification are found Figure 15.

The hardware is composed by:

- 1 Interface unit (Ascension DriveBAY™ and Aurora SIU): it is the integrated tracking unit that connects the computer to the transmitter and the sensors. It is responsible for the amplification and digitalization of the signals from the sensors, and for the control of the field generator.

- 1 Magnetic Field Generator (Ascension Mid-Range Transmitter and Aurora Planar Field Generator): this unit generates the electromagnetic field that defines the tracking volume of the system. The transmitter is positioned within 50cm from the operating environment so that it can be used in the normal mode avoiding loss of accuracy,

- 2 Sensors (in the Ascension set-up): the sensor used for the tracking of the needle is the *Model 130*, while the sensor for the displacement correction is the *Model 800*.

- 1 Probe (in the Aurora set-up): it is a general-purpose probe with a rigid straight metal tip for 6DoF for tracking.

driveBAY™

Mid-Range Transmitter

Specifications	
Accuracy	1.4 mm RMS 0.5 degrees RMS
Measurement Rate	user-configurable 20-255 Hz
Number of Sensors	4 (6DoF per unit)

Specifications	
Max. Tracking Distance (with *Model 800*)	Normal Mode: 660 mm Expanded Mode*: 1800 mm *Reduced specifications

Sensor Model 130

Sensor Model 800

Specifications	
Sensor OD	1.5 mm
Cable OD	1.2 mm
Sensor Lenght	7.7 mm
Cable Lenght	3.3 m

Specifications	
Sensor OD	7.9 mm
Cable OD	3.8 mm
Sensor Lenght	19.8 mm
Cable Lenght	3.3 m

Figure 14: Ascension 3D Guidance® Specifications
The image shows the pictures and the specifications of Ascension 3D Guidance® System hardware components that have been used.

Sensor Interface Unit (SIU)

Specifications	
Accuracy	0.48 mm RMS 0.3 degrees RMS
Measurement Rate	40 Hz
Number of Sensors	3 (6DoF per unit)

Planar Field Generator

Specifications	
Max. Tracking Distance	Cube Mode: 500 mm Dome Mode*: 660 mm *Reduced specifications

6DoF Probe

Specifications	
Tip Lenght	65 mm
Tip Diameter	3 mm

Figure 15: NDI Aurora Tools and Sensor Specifications
The image shows the pictures and the specification of NDI hardware components that have been used.

4.2.2 Monitor

The system has been implemented in order to work both with 2D or 3D monitor. The 3D visualization is implemented thanks to side-by-side 3D rendering in *LACE library*. When the 3D rendering is active, the rendering of the 3D objects is done with two different cameras. Each camera is displaced from the other by a distance defined as *eye separation*, and an asymmetric frustum of the cameras is defined to have an off-axis projection. The result is that the objects at the focal distance are seen in the same way by the two cameras, while increasing the distance from this plane, the objects will be seen from different angles by the two cameras.

The two camera views are rendered side by side in the screen with the left and right camera respectively on the left and right side of the screen. The 3D monitor fuses the two rendering, displaying each rendering with different rotational polarization; using the specific filtering glasses it is possible to see the right and left view only with the correspondent eye.

Since the eye separation is a parameter dependent on the position of the user respect to the screen, this parameter can be tuned in real-time in order to minimize the ghosting effect and maximize the 3D rendering efficacy.

4.2.3 Phantom

During the test in Chicago, a physical object has been used in order to test the system giving the urologists a more realistic experience. The phantom has to mimic the tissue elastic properties, offering the possibility for the user to mimic the biopsy procedure. For this purpose a block clear ballistic gel[61] has been chosen (Figure 16).

The clear ballistic gel is a material born with the purpose to simulate the human tissues during firing simulation, but it has found application also in medical simulations. The main advantage of this material is that it is transparent, so it allows the possibility to see the track of the needle even after the needle is removed[62].

For the testing, fiducial markers for the registration have been attached to the ballistic gel block. The position of the markers is known, and they have been reproduced in the 3D

environment in order to compensate for the absence of the fiducials during the acquisition of images.

Figure 16: Ballistic Gel Phantom
The image shows the ballistic gel block used to test the system. The dimension of the block, 21x21x20cm, is sufficient to contain a mean pelvis MRI volume.

4.3 SOFTWARE IMPLEMENTATION

The platform and the hardware described in the previous sections have been used in order to develop the *VRPBx* application, a software application for the *Virtual Reality Navigation System for Prostate Biopsy*. The application performs three tasks:

- Registration: registration of the anatomical image to the patient physical position according to the EMTS.
- Navigation: display of real-time virtual images for the execution of targeted biopsy.
- Evaluation: display of data and images useful to evaluate the surgery performance.

The following sections explain how those tasks have been implemented in the *VRPBx* application.

4.3.1 REGISTRATION

The registration is the process of finding the transform matrix between the virtual coordinate system of the anatomical data, and the coordinate system of the EMTS. In order to find the transformation, it is necessary to have some fiducial markers whose coordinates are known in both the coordinate systems. The fiducial markers are scanned with the patient during the image acquisition so that their virtual coordinates can be easily determined. The coordinates in the EMTS coordinate system are obtained before starting the procedure by touching the markers with the needle and storing the measured coordinates. During the registration, As shown in Figure 17, the graphic interface shows the position of the markers indicating in green which marker has to be acquired next.
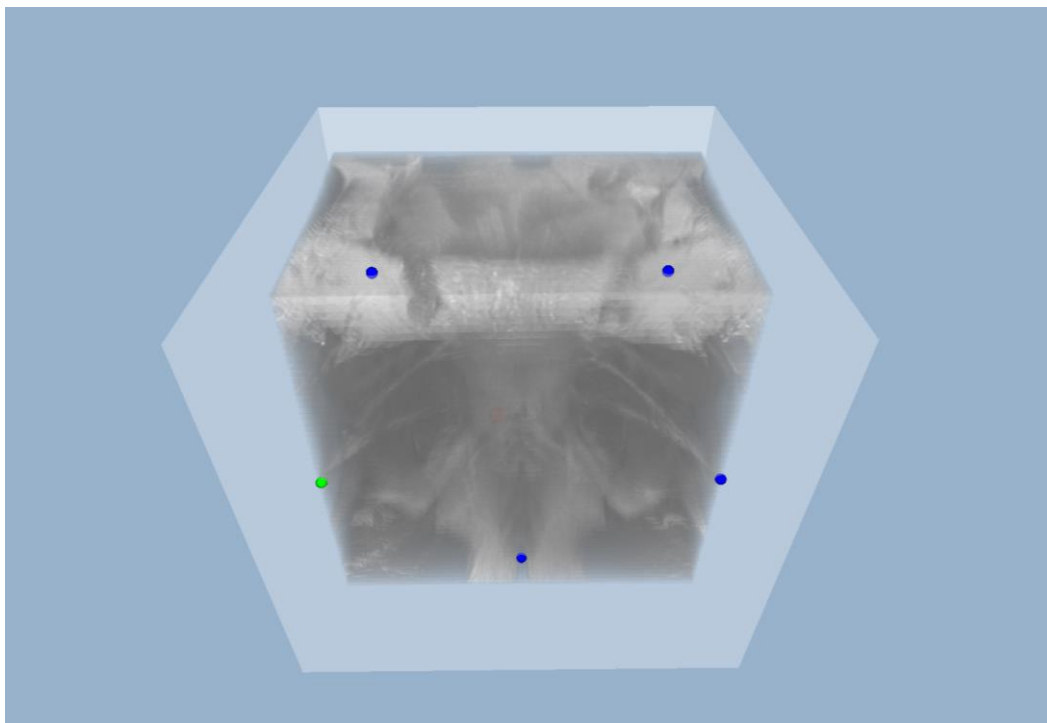
Figure 17: VRPBx Registration
During the registration process, the markers position of the markers is shown with blue dots. The green dot represents the fiducial point that has to be registered next.

After the data acquisition, an algorithm for paired-point rigid transform registration has been used to obtain the transform matrix that moves one system to the other. The choice of using a rigid transform is due to the fact that the choice of the markers position can minimize the

deformation between the patient pelvis before and during the procedure. Besides, it is not used the TRUS that is a main cause of deformation.

The algorithm used to determine the transformation matrix is based on the least-square error minimization, it is described in literature and widely used in medical application [63]. The demonstration of the algorithm is given in the Appendix A, while the algorithm is explained below.

Once the position of the fiducial points is known in both the coordinate systems, the algorithm runs the following steps:

- From the points coordinates $P = \{\mathbf{p_1}, \mathbf{p_2}, \dots, \mathbf{p_N}\}$ and $Q = \{\mathbf{q_1}, \mathbf{q_2}, \dots, \mathbf{q_N}\}$, the centroids of the distributions are computed:

$$\overline{\mathbf{p}} = \frac{\left(\sum_{i=1}^{N} \mathbf{p_i}\right)}{N}, \overline{\mathbf{q}} = \frac{\left(\sum_{i=1}^{N} \mathbf{q_i}\right)}{N} \tag{4.1}$$

- The covariance of the two distribution is computed:

$$H = \sum_{i=1}^{N} (\mathbf{p_i} - \overline{\mathbf{p}}) \cdot (\mathbf{q_i} - \overline{\mathbf{q}})^T \tag{4.2}$$

- The covariance matrix is decomposed using the Singular Value Decomposition (SVD).

$$[U, S, V] = SVD(H) \tag{4.3}$$

- The rotation matrix (R) is computed as:

$$R = V \cdot U^T \tag{4.4}$$

- If $det(VU^T) = -1$ the found rotation contains also a reflection. To obtain a simple rotation the last row of R is multiplied by -1.
- Finally, the translation (**t**) is computed as:

$$\mathbf{t} = \overline{\mathbf{q}} - R \cdot \overline{\mathbf{p}} \tag{4.5}$$

The rotation matrix (R) and the translation vector (**t**), describe the rigid transform that links the two coordinate systems.

To achieve this task, an additional library for linear algebra is required in order to have an efficient computation of the SVD. The chosen library is Eigen[64], a C++ template library for linear algebra, that implements the two-sided Jacobi iteration method to compute the SVD[65].

Rigid transform correction

The *correction sensor* is used to track the displacement of the pelvis that happens during the intervention. At the end of the registration process, the position of the "correction sensor" is stored; from this moment on, the sensor registers all the displacements correcting the translation matrix (R) and the rotation vector (**t**) computed in equations (4.4) and (4.5):

4.3.2 NAVIGATION

After the registration process, the position and orientation of the biopsy gun in the 3D virtual environment are known. This is possible since the *needle sensor* constantly tracks the biopsy gun, and the *correction sensor* measures the pelvis displacements.

The information regarding the needle position and the patient anatomy are combined in order to provide the surgeon a system of virtual images for the navigation. Figure 18 shows how the interface appears during this step, in the monitor the urologist has both a 3D virtual environment and the 2D orthogonal projections of the volume.

In order to not overload the surgeon, the visualization offered by the system is automatically setted and optimized; anyway, some parameters can be real-time tuned by the user through an intuitive graphic user interface (GUI) according to environmental requirements and personal preferences.
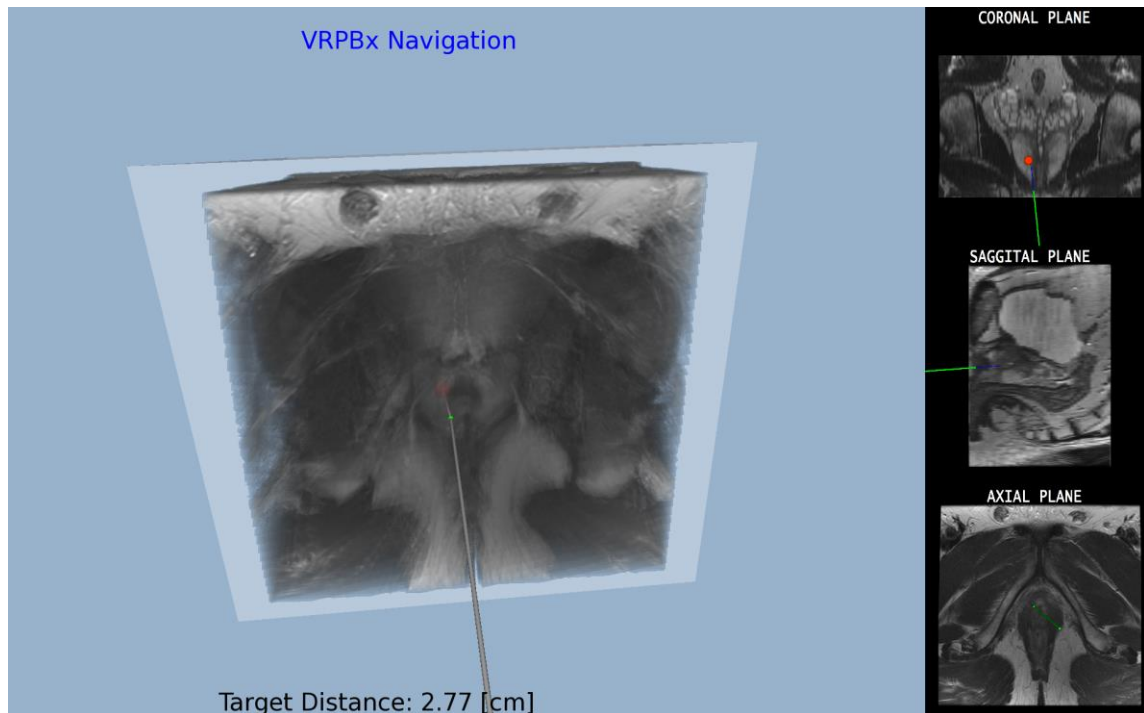
Figure 18: VRPBx Navigation Interface
During the navigation on the left of the screen a 3D virtual environment displays the volumetric anatomical information, the position of the needle and the target point together with other navigation features. On the right of the screen, three orthogonal plain of the volumetric image are displayed (Coronal Plane, Sagittal Plane, Axial Plane); the planes are taken in correspondence of the needle position. Also on the orthogonal planes a virtual needle is displayed, and the target point is displayed when it is on the active volume slice.

3D Environment

The 3D environment is the focus during the navigation and by default it fills the 80% of the screen. Figure 19 shows some of the possible rendering modality for this environment. For a better depth perception, a 3D monitor can be used in order to render it in 3D. The elements rendered in the 3D environment are:

- Patient volumetric image

The volumetric image can be rendered in the application with the three volume visualization modality offered by *LACE* (volumeSLICED, volumeRAYCAST, volumeORTHOGONAL).

- Mesh

Meshes segmented from the volumetric image can be loaded and rendered in order to simplify the detection of the organs for the urologist.

- Needle

The needle of the biopsy gun is shown in the environment accordingly to the position detected by the sensor. The tip of the needle is represented by a green dot, while, when the gun is loaded, the "shooting range" of the biopsy needle is represented as a transparent blue line that corresponds to the area in which the core will be taken. Figure 20 shows how the needle is rendered in the two cases.

- Target

One or more targets can be defined and visualized in order to perceive a targeted biopsy. The presence of a line, that connects the target and the tip of the needle, can facilitate the alignment of the biopsy needle with the target. In addition, the distance between the needle and the target is displayed on the screen.

- Core

Once the needle takes a sample the position of the taken core is stored and shown as a cylinder with the dimension corresponding to the core length (the visualization of the core during the navigation is the same as the one used during the evaluation shown in Figure 23)
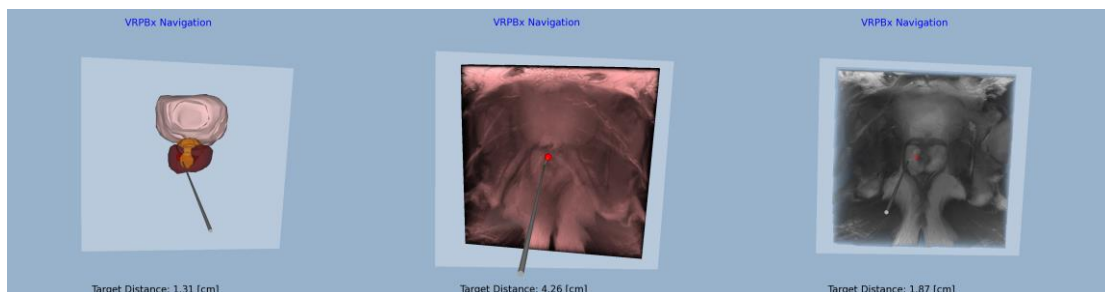

Figure 19: VRPBx Volume Rendering
During the navigation it is possible to visualize the mesh or to switch between different rendering modality for the volume. On the left only the meshes of the volume are displayed. On the middle, the volume is displayed as *LACE volumeRAYCAST*. On the right, the volume is displayed as *LACE volumeSLICED*.
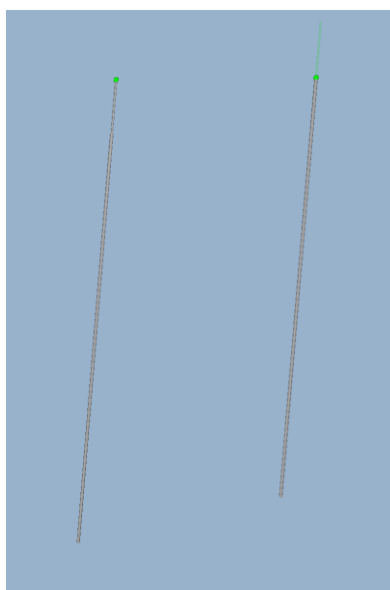
Figure 20: VRPBx Needle Rendering
During the navigation step the biopsy needle is constantly displayed on the screen as a grey cylinder and a green dot represent the tip of the needle. On the left it is represented the needle when the gun is not loaded, in this configuration the needle is not retracted. When the biopsy gun is loaded, the virtual needle appears as the one on the right of the picture, it retracted, and a transparent green line highlights the shooting range of the needle

2D Orthogonal Planes

The 20% right side of the monitor shows the three orthogonal slice of the MRI volume centered in the needle tip position. In those images, it is shown also the real-time position of the biopsy needle, and the eventual target of the biopsy.

The way the target is shown in the orthogonal planes is a sphere that appears only when the target is close to the visible slice; the color of the sphere indicates the distance from the slice in which the target lays (the color changes from yellow to red as the distance decrease).

As shown in Figure 21, it is also possible to focus on one of the projections.
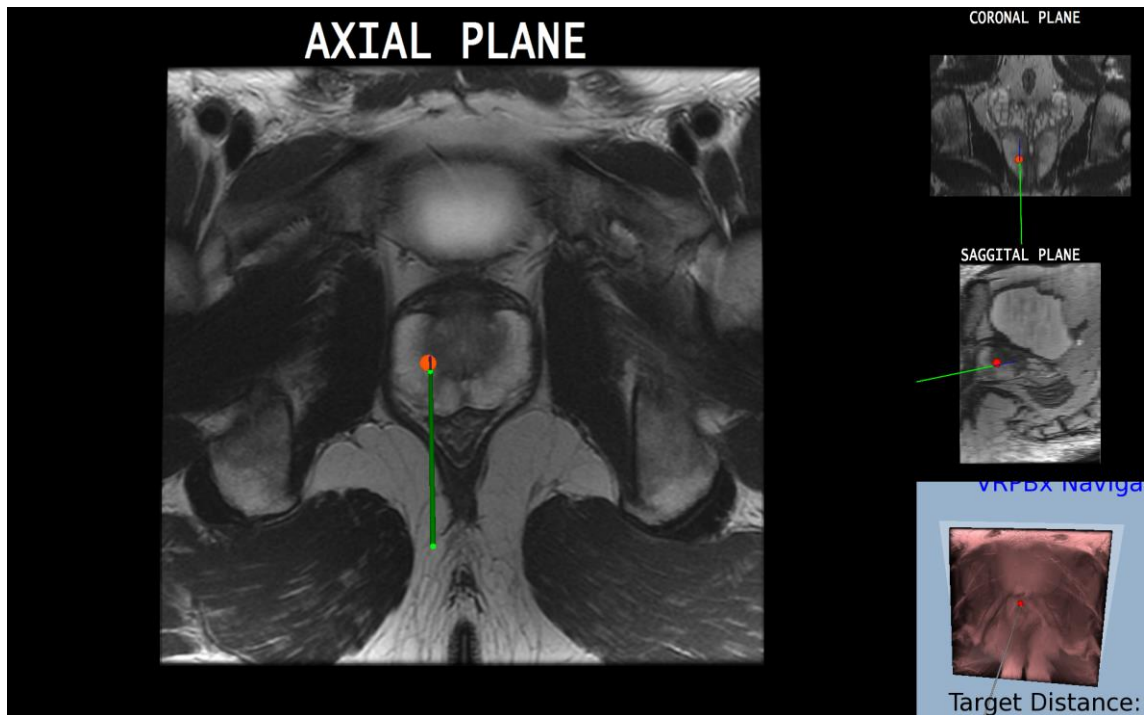
Figure 21: VRPBx Orthogonal Planes Zoom
During the navigation, the application allows the user to focus on one orthogonal plane that is visualized on the main viewport on the left.

Graphical User Interface (GUI)

The GUI is a window (Figure 22) that can be activate in order to set or tune the system parameters. The parameters that are controlled by the GUI are:

- Switch between the different steps (Registration, Navigation and Evaluation)
- Mesh and Volume parameters (visibility, rendering mode, transfer functions, bias)
- "Correction sensor" activation
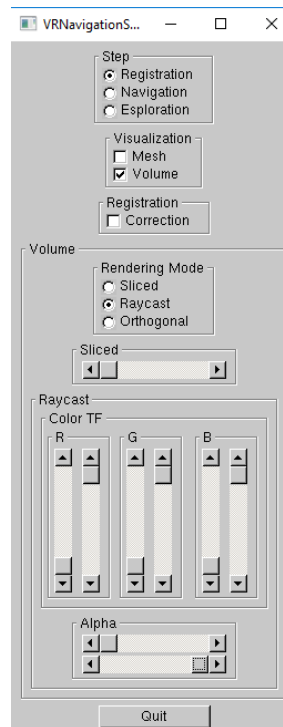
Figure 22: VRPBx GUI
In every moment, it is possible to open the GUI in order to set the system parameters. The GUI gives the possibility to select the step of the procedure, to activate the correction sensor, and to tune the parameter for volume and mesh visualization.

4.3.3 EVALUATION

In every moment during the procedure or at the end it is possible to observe in the 3D environment the position of the taken cores and read the distance of each core form the target to evaluate the coverage of the target point. Figure 23 shows the interface during this step.
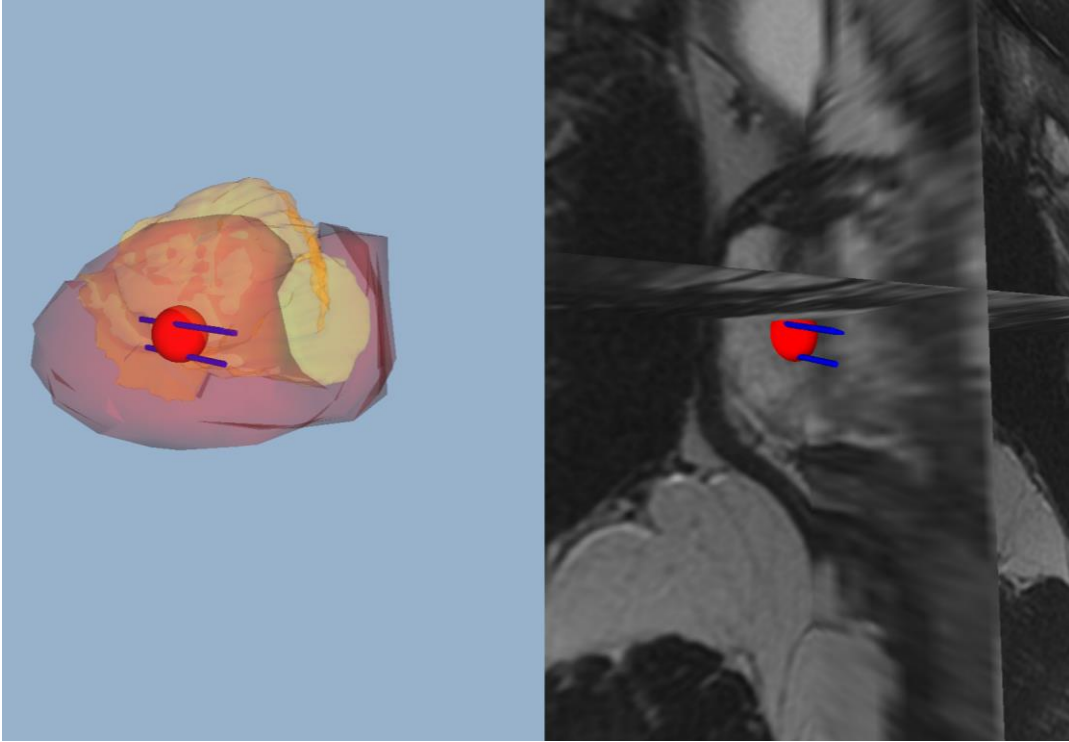
Figure 23: VRPBx Procedure Evaluation
The figure shows two examples of visualization to evaluate the biopsy performance. On the left the evaluation is done using the meshes, while on the right it is done using the MRI orthogonal planes. In red it is shown the target of the biopsy, while the blue cylinders represent the location where the samples have been taken.

5 EXPERIMENTAL EVALUATION AND RESULTS

5.1 SYSTEM ARCHITECTURE

The application presented in this thesis was firstly developed on a workstation available at the UIC, and it was used in order to have a preliminary evaluation of the system with the collaboration of the Department of Urology of the University of Illinois College of Medicine. After this step, the set-up has been reproduced and readapted at Politecnico di Milano in order to have more specific tests focused on the evaluation of the graphics interface. The main features of the two systems are reported in Table 1.

5.2 PRELIMINARY EVALUATION

The *virtual reality navigation system for prostate biopsy* has been discussed and tested in Chicago with experienced urology surgeons and faculties of the Department of Urology. For this preliminary test step, the aim was to have a feedback on the feasibility of the set-up in clinical practice, and on the quality of the graphics interface from an experts' point of view. During the test sessions, they have had the opportunity to use the navigation system performing registration and navigation on a ballistic gel phantom. Those tests offer them the

opportunity to observe the proposed graphic interface exploring the different modalities for guided and targeted navigation.

	UIC	POLIMI
Processor	Intel Core i5 – 2500K CPU 3.3GHz	Intel Core i7 – 3770K CPU 3.4GHz
RAM	8GB	8GB
GPU	NVIDIA Quadro K6000	NVIDIA TITAN Xp
Tracking System	Ascension 3D Guidance	NDI Aurora
Stereoscopic Display	YES	NO
Correction Sensor	YES	NO
Physical Phantom	YES	NO

Table 1: Main Features of Politecnico di Milano and UIC experimental set-up

5.3 GRAPHICS INTERFACE EVALUATION

After the preliminary evaluation of the navigation system, a study has been conducted in order to investigate the quality of the graphic interface offered by the application. The four areas of investigation are:

- Visual Rendering

  Performance of the system in rendering volume and meshes, and exploring the scene.

- Tracking

  Performance of the communication between the tracking system and the graphics interface.

- Anatomical Information

  Ease with which it is possible to get anatomical information of the patient from the 3D volumetric images.

- Guidance Assistance

    Features for the targeting assistance.

The study has been conducted at the Vialba Medical School of Università degli Studi di Milano at Sacco hospital.

5.3.1 EXPERIMENTAL PROTOCOL

For this study 26 medical students, attending at least their second year, have been recruited. Before starting a hands-on session, they have been shown all the steps of the application, and they have been thought all the possible action that can be done interacting with the system

After this introduction, they were asked to:

- Explore the MRI through the 3D interface
- Explore all the possible rendering modality
- Select a target
- Point the target with the cursor
- Observe the performance with the evaluation interface

At the end of the hands-on session, they were asked to fill a questionnaire for the assessment of the system. The questionnaire consists of 11 questions, that are either open or multiple choice (whose possible answers are reported in Table 2).

	Questions 4-5			*Questions 6-10*
1	Not at all		1	Very Poor
2	Somewhat		2	Below Average
3	Fairly		3	Average
4	Very		4	Above Average
5	Extremely		5	Excellent

Table 2: Multiple choice answers

The first questions have the aim to gather information about users' medical experience (statements 1-3), and their familiarity with virtual reality (multiple choice questions 4-5). Questions from 6 to 10 are multiple choice questions that allow subjects to rate their experience with the application. The last question is used to eventually obtain further general feedbacks. All the questionnaires were distributed in English, and explained for a better understanding, and the subjects were asked not to answer if they did not feel qualified to give an evaluation.

1	What is your current position?
2	Have you ever performed a prostate biopsy?
3	Have you ever been involved in virtual reality guided intervention?
4	How familiar are you with virtual reality
5	In general, would you feel comfortable in performing a surgery guided by virtual images?
	How would you evaluate the software in term of:
6	Visual Rendering
7	Tracking
8	Anatomical Information
9	Guidance Assistance
10	How would you evaluate the overall performance?
11	Do you have any comment or suggestion?

Table 3: Assessment questionnaire for the Prostate Biopsy Navigation System

5.3.2 RESULTS

This section reports the most significant results obtained from the *Assessment questionnaire for the Prostate Biopsy Navigation System* (Table 3).

Table 4 shows the results of mean, standard deviation and number of datas from the quantitative questions 4 to 10, while Figure 24 shows pie charts of the responses given by subjects to each of the questions strictly related to the software application (i.e., questions 6-10).

The mean score given to questions shows the application has been evaluated above average as performance. Moreover, even if most of the subjects do not evaluate themselves as familiar in virtual reality, they would feel comfortable in using virtual images as surgical guidance.

Questions	Data	Score
4.	27	2.11±1.01
5.	14	4.07±0.62
6.	27	3.77±0.76
7.	27	3.92±0.98
8.	27	3.92±0.77
9.	27	3.73±0.99
10.	26	3.88±0.83

Table 4: Mean score and SD of quantitative answers from assessment questionnaire
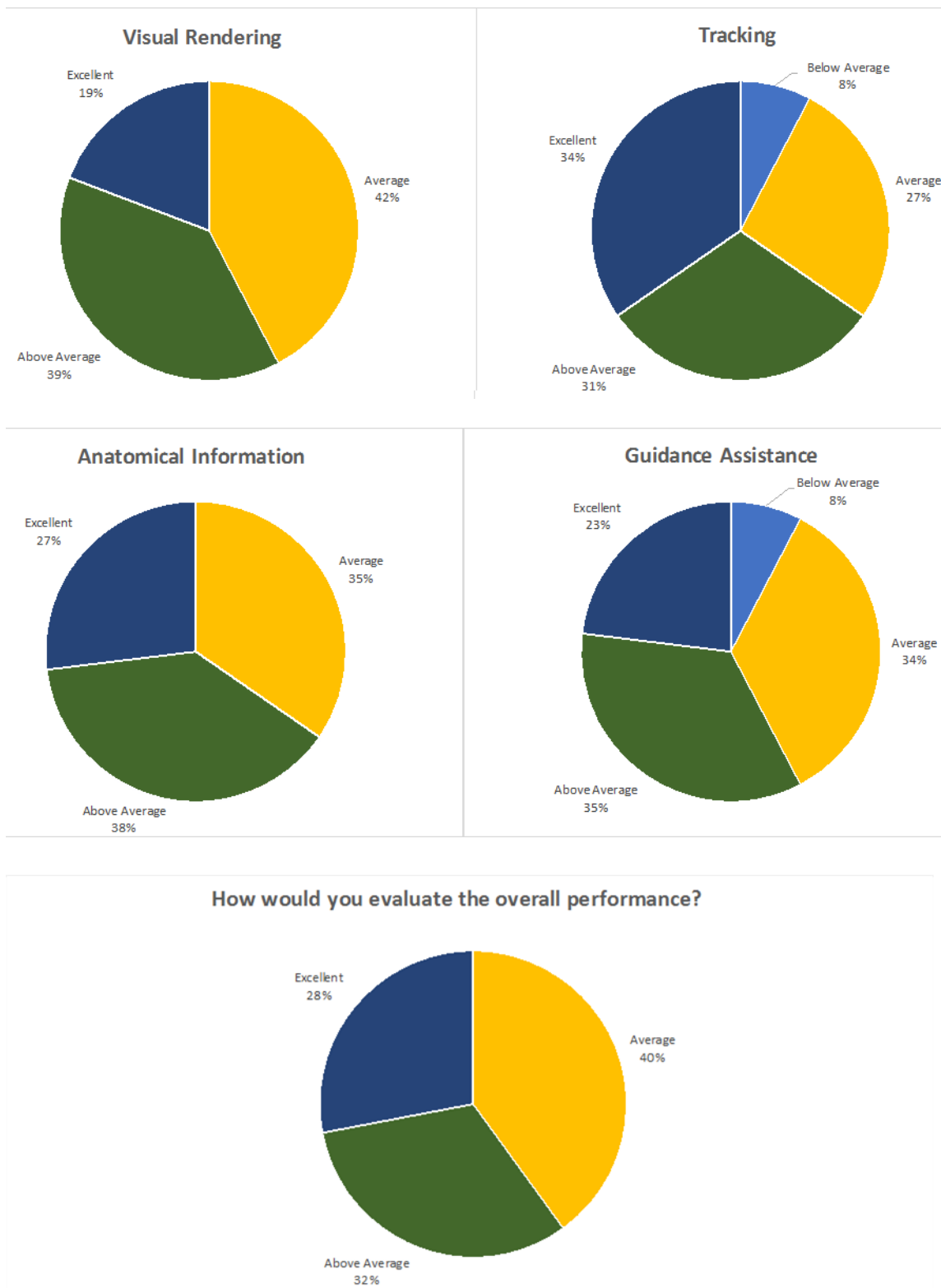
Figure 24: Pie charts of questionnaire responses
Responses to questions 6-10 of the assessment questionnaire for the Prostate Biopsy Navigation System.

5.4 DISCUSSION

The main objective of this thesis was the development of the prototype for an innovative navigation system for prostate biopsy that overcomes the weakness of the available navigation systems. Both biopsy needle and patient anatomy are constantly tracked by an electromagnetic tracking system that provides their 3D position and orientation with respect to the surgical bed. Multiple fiducial markers are placed on the patient skin (at the iliac crest and pubic bone) during MRI scanning. Once in the operative room, the surgeon is presented a stereoscopic 3D volumetric rendering and multiple orthogonal views of the patient anatomy, as well as a virtual representation of the tracked needle. After a simple registration process between the MRI and the tracker coordinate system, the navigation system guides the needle insertion in the patient perineum through several anatomical layers towards the biopsy targets. The surgeon can easily load volumetric images and interact with the interface exploring a combination of rendering modalities.

The creation of this virtual reality application, where both high-performance graphics and real-time tracking coexist, has been possible thanks to the implementation of *LACE library*. This C++ based library has proved to be a very intuitive and easy way to conjugate several software-hardware components that are needed to develop VR-based medical applications. It represents a flexible tool that has turned out to be adapt to the creation of a variety of virtual environments, like the ones proposed in [51][52][53].

During the procedure, a real-time visual feedback is provided to the surgeon through a stereoscopic 3D monitor. The graphic interface displays virtual images of needle and internal anatomy both using 3D rendering and multiple orthogonal view of the patient anatomy.The rendering of the volumetric image can be done with three different modalities: volume sliced, volume ray casting, and visualizing the three orthogonal planes centered on the needle tip. The transfer function and transparency can be interactively adjusted by the user. The system also provides the possibility to clip the volume with a plane in order to have a better view of internal anatomy. Furthermore, the navigation system gives the surgeon additional information to guide the surgeon accordingly to intraoperative performances and pre-operative planning. Those features include the position of the cores that were previously taken, the distance between the needle and the target, the shot range of the needle, and the

direction from the needle tip to the target point. The graphical interface is intuitive and flexible to adapt to patient condition and surgeon preferences. The information provided allows the surgeon to efficiently perform a targeted biopsy without an overload of information. The EMTS tracks the 3D position and orientation of the needle in the surgical field during the procedure replacing the TRUS for real-time tracking. The use of EMTS prevents the tissue deformation caused by the TRUS probe, minimizing the overall deformation. Moreover, with the TRUS the position of the needle is derived from the surrounding visible tissues only when the needle is in the visual field of the ultrasound. With the EMTS the position of the needle is always known once the registration is done. As consequence, the virtual reality navigation system for prostate biopsy offers a guidance not only when the needle is inside the patient anatomy, but also while the needle is outside the patient optimizing perineum access.

The virtual reality navigation system for prostate biopsy has been preliminary tested by a cohort of experienced urology surgeons using a ballistic gel phantom to perform the registration and navigation process, observing the proposed graphic interface exploring the different modalities for guided and targeted navigation. The urologists have underlined the weakness of systematic approach and MRI-TRUS image fusion techniques, for this reason they agree about the need of applying modern technologies to move towards intuitive and easy-to-use methods for targeted biopsy expressing enthusiasm in the possibility to replace the TRUS with the proposed tracking technique. They have observed that the proposed graphical interface offers a complete anatomical information for prostate biopsy navigation thanks to the combination of a 3D environment with the 2D orthogonal views. The enhanced virtual visual feedback gives the surgeon the opportunity of performing a targeted biopsy with short pre-processing time, guided by a simple interface. Furthermore, they have positively highlighted the unique opportunity offered by the system to aligning the needle with the target before inserting it through the perineum significantly reducing the surgical time. The main challenge they see is the possible displacement of the prostate from pre-operative conformation due to muscles contraction, however they stated that it should not be a problem for non-small lesions (>1ml). They have also discussed about whether the system should include a template as support and guidance, but they agreed that it could be a possibility, but the final step should be to get the biopsy done with no template at all which will make the set up for the procedure shorter and less expensive. Another option they have

carried on is the possibility to use the coaxial needle technique in case multiple samples are required, and it consist in using a bigger and shorter hollow needle to enter the skin and guide the real biopsy needle to the target as it is already used for standard transperineal biopsies.

The application interface has been evaluated by a cohort of 26 medical students of Università degli Studi di Milano through an assessment questionnaire. Pie charts in Figure 24 shows the results for the questions 6 to 10 that are the main statements of the questionnaire, and for all those five categories the subjects evaluated the application above average. It was also helpful to gather additional feedback and suggestions from the subjects. Overall they were enthusiastic about the possibility offered by the interface to navigate the MRI and being supported in the targeting through a virtual reality interface, even if in most of the case they were not familiar with virtual reality. This highlights an open-mind and desire for including new technologies in the medical field. The main difficulty they encountered was related to the depth perception, since they didn't have the opportunity to use the 3D display. Other improvements that have been suggested were the possibility to have a stronger visual guidance, and eventually a physical guidance as a haptic feedback. Thanks to *LACE* functionalities, it will be possible to work at those improvements including the use of the haptic feedback.

6 CONCLUSIONS

This thesis describes the development of the application and the prototype for a navigation system for prostate biopsy based on the electromagnetic tracking of the needle and MRI, designed to overcome the weakness of state of the art navigation system for prostate biopsy. It propose an innovative and unique approach for prostate biopsy combining an EMTS and virtual reality to replace the traditional TRUS real-time instrument guidance. Its realization exploits also the functionality of an efficient and novel C++ based platform, *LACE library*, which has been implemented to facilitate the integration of software-hardware components in development of mixed-reality based application.

The proposed system is the *virtual reality navigation system for prostate biopsy*, an innovative and unique approach for prostate biopsy procedure. The navigation relies on virtual images that are obtained through the registration of the tracked needle to MRI. The system has been designed, under the advise of expert urologists, in all of its software/hardware components and successfully underwent through a preliminary evaluation. The goal was to achieve not only an accurate safe and comfortable system for the patient, but also an intuitive easy-to-use instrument for surgeons.

In the prototype that I have developed, the traditional TRUS real-time instrument guidance has been successfully replaced by the EMTS that constantly determine the position of the needle in the operating environment. The anatomical information is obtained from the MRI, or equivalent volume imaging techniques that can detect suspicious regions to be targeted during the biopsy. The 3D graphic interface fuses the anatomical model with the needle tracking and, together with the orthogonal projection of the volume, constitutes a valid instrument for pelvis navigation.

The application has demonstrated having an interface able to offer a concrete help to the surgeon for the targeting of suspicious areas, ensuring good performance in term of graphics rendering and tracking. Furthermore, the preliminary results presented in this works highlight the importance of exploring non-TRUS based navigation systems and the possible role that they could have into the near future.

As a collateral result of this project, *LACE library* has been implemented and tested in collaboration with other researchers of the Mixed Reality Lab, proving to be a valid

instrument for software development. The performance of the library were satisfactory with the requirements of the application, and, in particular, *LACE* efficiently controls the communication between the 3D tracking system (EMTS) and a high-performance OpenGL library for 3D graphic rendering. The performance of *LACE* has been tested for what regards the haptics rendering in three other applications[51][52][53], and also in those cases it gave satisfying results, granting a perfectly distributed computer load between real-time haptics and 3D graphics.

6.1 FUTURE DEVELOPMENT

Even though some preliminary experiments have been done, it is necessary to conduct a more accurate validation of the system in order to evaluate the usability in clinical practice.

The first step that is required is the analysis of the system accuracy. There are different factors that characterize the overall system accuracy, a study of all those components individually is important in order to define and optimize some design features of the system. In order to complete this analysis, it is necessary have an experimental set-up with a reliable pelvis phantom, so that it is possible to scan the phantom with the fiducials, register the position of the phantom, perform the biopsy on elastic tissues, and evaluate the targeting error between the real and the virtual world. Accordingly to literature, the required target registration error for targeting small lesions is <1.9mm[50], but even with lower level of accuracy the system could be an instrument to target larger suspicious areas (e.g. >1ml):

In parallel to the accuracy assessment, it will be necessary to move through different prototypes focusing on specific elements of the system. The most relevant open questions regards: the fiducial markers positioning, the sensor needle integration and the patient positioning. Another possible development could be the integration of some additional information such as the fusion of different imaging techniques, or the implementation of different rendering techniques.

For what concerns the graphics interface, some further studies can be done in the future with a larger sample of expert surgeons. Furthermore, the same interface could be implemented for different surgical procedure for a wider study about virtual reality in surgical navigation.

Today *LACE* is being introduced as developing platform for different projects concerning the combination of haptics, 3D rendering and tracking. Further improvements can be done by integrating the communication with new technologies for virtual reality such as head-mounted display or other haptics technologies. It is also necessary to produce a detailed documentation and a set of sample applications in order to make the library available and easy to use for students and researchers.

APPENDICES

APPENDIX A

PAIRED-POINTS LEAST-SQUARE DEMONSTRATION

Given the N fiducial points, $P = \{\mathbf{p_1}, \mathbf{p_1}, \dots, \mathbf{p_N}\}$ is the vector with the coordinates in the virtual coordinate system, while $Q = \{\mathbf{q_1}, \mathbf{q_1}, \dots, \mathbf{q_N}\}$ is the vector with the coordinates in the tracker coordinate system.

In the ideal case the transform is composed by a rotation matrix R and a vector $\mathbf{t}$ so that for each point:

$$\tilde{\mathbf{q}}_\mathbf{i} = R\mathbf{p_i} + \mathbf{t} \qquad \forall i = 1 \dots N \qquad (A.1)$$

where $\hat{\mathbf{q}}_\mathbf{i}$ is the ideal coordinate of the point in the real coordinate system.

Since the position measured with the tracker is not ideal and the tissue can be deformed between the MRI acquisition and the point registration, an error is present:

$$\mathbf{q_i} = \tilde{\mathbf{q}}_\mathbf{i} + \boldsymbol{\varepsilon}_i \qquad \forall i = 1 \dots N \qquad (A.2)$$

According to the least-square algorithm, the matrix R and a vector $\mathbf{t}$ are those that minimize the summed squared error, replacing the error $\boldsymbol{\varepsilon}_i$ accordingly to equations (A.1) and (A.2) their value is obtained by minimizing the objective function:

$$(R, \mathbf{t}) = \mathrm{argmin}_{R,\mathbf{t}} \sum_{i=1}^{N} \|\boldsymbol{\varepsilon}_i\|^2 = \mathrm{argmin}_{R,\mathbf{t}} \sum_{i=1}^{N} \|(R\mathbf{p_i} + \mathbf{t}) - \mathbf{q_i}\|^2 \qquad (A.3)$$

Assuming R is fixed, the translation is determined finding the roots of the summed squared error derivative:

$$0 = \frac{\partial\left[\sum_{i=1}^{N}\|(R\mathbf{p_i} + \mathbf{t}) - \mathbf{q_i}\|^2\right]}{\partial \mathbf{t}} =$$

$$= 2N \cdot \mathbf{t} + 2R\left(\sum_{i=1}^{N} \mathbf{p_i}\right) - 2\left(\sum_{i=1}^{N} \mathbf{q_i}\right) \qquad (A.4)$$

Defining the centroid $\bar{\mathbf{p}}$ and $\bar{\mathbf{q}}$ of the two vectors of point, the equation (A.5) can be written as:

$$N \cdot \mathbf{t} + R \cdot (N \cdot \bar{\mathbf{p}}) - (N \cdot \bar{\mathbf{q}}) = 0 \qquad (A.5)$$

where the centroids are:

$$\bar{\mathbf{p}} = \frac{\left(\sum_{i=1}^{N} \mathbf{p_i}\right)}{N}, \bar{\mathbf{q}} = \frac{\left(\sum_{i=1}^{N} \mathbf{q_i}\right)}{N} \tag{A.6}$$

Rearranging the equation (A.5) the optimal $\mathbf{t}$ is explicated as:

$$\mathbf{t} = \bar{\mathbf{q}} - R \cdot \bar{\mathbf{p}} \tag{A.7}$$

The optimal $\mathbf{t}$ obtained in equation (A.7) can be plugged in the objective function (A.3):

$$\sum_{i=1}^{N} \|(R\mathbf{p_i} + \mathbf{t}) - \mathbf{q_i}\|^2 = \sum_{i=1}^{N} \|(R \cdot (\mathbf{p_i} - \bar{\mathbf{p}}) - (\mathbf{q_i} - \bar{\mathbf{q}})\|^2 \tag{A.8}$$

Given (A.8), the rotation R can be found by restarting the problem from (A.3) with the vector $\mathbf{t}$ equal to zero:

$$\hat{\mathbf{p_i}} := \mathbf{p_i} - \bar{\mathbf{p}}, \qquad \hat{\mathbf{q_i}} := \mathbf{q_i} - \bar{\mathbf{q}} \qquad \forall i = 1 \dots N$$

$$R = \operatorname*{argmin}_R \sum_{i=1}^{N} \|(R\mathbf{p_i} + \mathbf{t}) - \mathbf{q_i}\|^2 = \operatorname*{argmin}_R \sum_{i=1}^{N} \|R\hat{\mathbf{p}}_i - \hat{\mathbf{q}}_i\|^2 \tag{A.9}$$

The argoument of equation (A.9) can be expanded and simplified remembering that a rotation matrix by definition is an orthogonal matrix ($R^T R = RR^T = I$), and that for a scalar $a^T = a$:

$$\|R\hat{\mathbf{p}}_i - \hat{\mathbf{q}}_i\|^2 = (R\hat{\mathbf{p}}_i - \hat{\mathbf{q}}_i)^T (R\hat{\mathbf{p}}_i - \hat{\mathbf{q}}_i) = \left(\hat{\mathbf{p}}_i^T R^T - \hat{\mathbf{q}}_i^T\right)(R\hat{\mathbf{p}}_i - \hat{\mathbf{q}}_i)$$

$$=$$

$$= \hat{\mathbf{p}}_i^T R^T R \hat{\mathbf{p}}_i - \hat{\mathbf{q}}_i^T R \hat{\mathbf{p}}_i - \hat{\mathbf{p}}_i^T R^T \hat{\mathbf{q}}_i + \hat{\mathbf{q}}_i^T \hat{\mathbf{q}}_i =$$

$$= \hat{\mathbf{p}}_i^T \hat{\mathbf{p}}_i - \hat{\mathbf{q}}_i^T R \hat{\mathbf{p}}_i - \hat{\mathbf{p}}_i^T R^T \hat{\mathbf{q}}_i + \hat{\mathbf{q}}_i^T \hat{\mathbf{q}}_i = \tag{A.10}$$

$$= \hat{\mathbf{p}}_i^T \hat{\mathbf{p}}_i - \hat{\mathbf{q}}_i^T R \hat{\mathbf{p}}_i - (\hat{\mathbf{p}}_i^T R^T \hat{\mathbf{q}}_i)^T + \hat{\mathbf{q}}_i^T \hat{\mathbf{q}}_i =$$

$$= \hat{\mathbf{p}}_i^T \hat{\mathbf{p}}_i - 2 \cdot \hat{\mathbf{q}}_i^T R \hat{\mathbf{p}}_i + \hat{\mathbf{q}}_i^T \hat{\mathbf{q}}_i$$

Plugging the result of equation (A.10) in the minimization problem of equation (A.9), the terms that do not depend on R can be eliminate:

$$R = \text{argmin}_R \sum_{i=1}^{N} \|R\hat{\mathbf{p}}_i - \hat{\mathbf{q}}_i\|^2 =$$

$$= \text{argmin}_R \sum_{i=1}^{N} (\hat{\mathbf{p}}_i{}^T\hat{\mathbf{p}}_i - 2 \cdot \hat{\mathbf{q}}_i{}^T R\hat{\mathbf{p}}_i + \hat{\mathbf{q}}_i{}^T\hat{\mathbf{q}}_i) =$$

$$= \text{argmin}_R \sum_{i=1}^{N} (-2 \cdot \hat{\mathbf{q}}_i{}^T R\hat{\mathbf{p}}_i) = \tag{A.11}$$

$$= \text{argmin}_R \left[-2 \cdot \sum_{i=1}^{N} (\hat{\mathbf{q}}_i{}^T R\hat{\mathbf{p}}_i) \right] = \text{argmax}_R \sum_{i=1}^{N} (\hat{\mathbf{q}}_i{}^T R\hat{\mathbf{p}}_i)$$

Collecting the N vectors $\hat{\mathbf{q}}_i$ and $\hat{\mathbf{p}}_i$ in two matrices $\hat{Q}$ and $\hat{P}$:

$$\hat{Q} = \begin{bmatrix} | & | & & | \\ \hat{\mathbf{q}}_1 & \hat{\mathbf{q}}_2 & \cdots & \hat{\mathbf{q}}_N \\ | & | & & | \end{bmatrix} \quad \hat{P} = \begin{bmatrix} | & | & & | \\ \hat{\mathbf{p}}_1 & \hat{\mathbf{p}}_2 & \cdots & \hat{\mathbf{p}}_N \\ | & | & & | \end{bmatrix}$$

$$Q^T RP = \begin{bmatrix} \hat{\mathbf{q}}_1{}^T R\hat{\mathbf{p}}_1 & & & * \\ & \hat{\mathbf{q}}_2{}^T R\hat{\mathbf{p}}_2 & \cdots & \\ * & & & \hat{\mathbf{q}}_N{}^T R\hat{\mathbf{p}}_N \end{bmatrix} \tag{A.12}$$

So from equation (A.12) the quantity that has to me maximized is $\sum_{i=1}^{N}(\hat{\mathbf{q}}_i{}^T R\hat{\mathbf{p}}_i) = tr(\hat{Q}^T R\hat{P})$, the equation (A.11) can be written as:

$$R = \text{argmax}_R \sum_{i=1}^{N} (\hat{\mathbf{q}}_i{}^T R\hat{\mathbf{p}}_i) = \text{argmax}_R tr(\hat{Q}^T R\hat{P}) \tag{A.13}$$

For the property of matrix trace, $tr(AB) = tr(BA)$ if the two matrices have same dimension. Defining the covariance matrix $S = \hat{P}\hat{Q}^T$, and its SVD $S = U\Sigma V^T$, the equation (A.13) becomes:

$$R = \text{argmax}_R tr(\hat{Q}^T R\hat{P}) = \text{argmax}_R tr(R\hat{P}\hat{Q}^T) = \text{argmax}_R tr(RS) =$$

$$= \text{argmax}_R tr(RU\Sigma V^T) = \text{argmax}_R tr(\Sigma V^T RU) \tag{A.14}$$

The matrix $M = V^T RU$ is an orthonormal matrix since V, R and U are orthonormal, while Σ is a diagonal matrix with non-negative values. Therefore:

$$tr(\Sigma V^T RU) = tr(\Sigma M) = tr\left[\begin{pmatrix} \sigma_1 & & \\ & \sigma_2 & \dots \\ & & \sigma_d \end{pmatrix}\begin{pmatrix} m_{11} & \cdots & m_{1d} \\ \vdots & \ddots & \vdots \\ m_{d1} & \cdots & m_{dd} \end{pmatrix}\right] = \tag{A.15}$$

$$= \sum_{i=1}^{d} \sigma_i m_{ii} \le \sum_{i=1}^{d} \sigma_i$$

where d is the dimension of the covariance matrix S, and σ_i are the values on the diagonal of Σ ($\sigma_i \ge 0 \; \forall i = 1 \dots d$). The last step of equation (A.15) is achieved because $|m_{ij}| \le 1$.

Therefore $tr(\Sigma V^T RU)$ is maximized when $\sum_{i=1}^{d} \sigma_i m_{ii} = \sum_{i=1}^{d} \sigma_i$, which means that $m_{ii} = 1$ and so M is an identity matrix:

$$\begin{matrix} M = I \\ M = V^T RU \end{matrix} \Rightarrow V = RU \Rightarrow R = VU^T \tag{A.16}$$

The obtained rotational matrix R can be both a simple rotation or can contains also a reflection. The second case happens when $det(VU^T) = -1$. Since a reflection matrix can be constructed from a rotation matrix by inverting the sign of a row and vice versa, in case of $det(VU^T) = -1$, the solution for the simple rotation is:

$$R = V\begin{pmatrix} 1 & & \\ & 1 & \dots \\ & & -1 \end{pmatrix}U^T \tag{A.17}$$

that corresponds to changing the sign of the last row of R.

CITED LITERATURE

[1]   "United States Cancer Statistics." [Online]. Available: https://nccd.cdc.gov/uscs/. [Accessed: 26-Mar-2017].

[2]   R. L. Siegel, K. D. Miller, and A. Jemal, "Cancer statistics," *CA Cancer J Clin*, vol. 66, no. 1, pp. 7–30, 2016.

[3]   E. C. Serefoglu, S. Altinova, N. S. Ugras, E. Akincioglu, E. Asil, and M. D. Balbay, "How reliable is 12-core prostate biopsy procedure in the detection of prostate cancer?," *Can. Urol. Assoc. J.*, vol. 7, no. 5–6, pp. E293-8, 2013.

[4]   L. Marks, S. Young, and S. Natarajan, "MRI-ultrasound fusion for guidance of targeted prostate biopsy.," *Curr. Opin. Urol.*, vol. 23, no. 1, pp. 43–50, 2013.

[5]   U. Mezger, C. Jendrewski, and M. Bartels, "Navigation in surgery," *Langenbeck's Arch. Surg.*, vol. 398, no. 4, pp. 501–514, 2013.

[6]   I. S. C. Verploegh *et al.*, "Contemporary frameless intracranial biopsy techniques: Might variation in safety and efficacy be expected?," *Acta Neurochir. (Wien).*, vol. 157, no. 11, pp. 2011–2016, 2015.

[7]   C. H. Lee, O. Akin-Olugbade, and A. Kirschenbaum, "Overview of Prostate Anatomy, Histology, and Pathology," *Endocrinol. Metab. Clin. North Am.*, vol. 40, no. 3, pp. 565–575, 2011.

[8]   "Prostate Anatomy: Overview, Gross Anatomy, Microscopic Anatomy." [Online]. Available: http://emedicine.medscape.com/article/1923122-overview#a2. [Accessed: 26-Mar-2017].

[9]   "Benign Prostatic Hyperplasia: American Urological Association." [Online]. Available: https://www.auanet.org/education/benign-prostatic-hypertrophy.cfm. [Accessed: 26-Mar-2017].

[10]   "Prostate - Anatomy Pictures and Physiology." [Online]. Available: http://www.innerbody.com/image_repmov/repo09-new4.html. [Accessed: 26-Mar-2017].

[11]   M. Andreoiu and L. Cheng, "Multifocal prostate cancer: biologic, prognostic, and therapeutic implications," *Hum. Pathol.*, vol. 41, no. 6, pp. 781–793, 2010.

[12]   S. Loeb and W. J. Catalona, "What to do with an abnormal PSA test.," *Oncologist*, vol. 13, pp. 299–305, 2008.

[13]   "WebMD - Better information. Better health." [Online]. Available: http://www.webmd.com/. [Accessed: 26-Mar-2017].

[14]   F. H. Schro, P. Van Der, P. Beemsterboer, B. Kruger, and J. Rietbergen, "Evaluation of the Digital Rectal Examination as a Screening Test for Prostate Cancer," vol. 90, no. 23, pp. 1817–1823, 1998.

[15]   "Comprehensive Cancer Information - National Cancer Institute." [Online]. Available: https://www.cancer.gov/. [Accessed: 26-Mar-2017].

[16]   R. M. Hoffman, F. D. Gilliland, M. Adams-Cameron, W. C. Hunt, and C. R. Key, "Prostate-specific antigen testing accuracy in community practice.," *BMC Fam.*

Pract., vol. 3, p. 19, 2002.

[17] S. Ghai and A. Toi, "Role of Transrectal Ultrasonography in Prostate Cancer," *Radiol. Clin. North Am.*, vol. 50, no. 6, pp. 1061–1073, 2012.

[18] G. Salomon *et al.*, "Evaluation of Prostate Cancer Detection with Ultrasound Real-Time Elastography: A Comparison with Step Section Pathological Analysis after Radical Prostatectomy," *Eur. Urol.*, vol. 54, no. 6, pp. 1354–1362, 2008.

[19] S. Ikonen, L. Kivisaari, P. Tervahartiala, T. Vehmas, K. Taari, and S. Rannikko, "Prostatic MR imaging. Accuracy in differentiating cancer from other prostatic disorders.," *Acta radiol.*, vol. 42, no. 4, pp. 348–354, 2001.

[20] P. Kang, M. Liao, M. R. Wester, J. S. Leeder, and R. E. Pearce, "Multiparametric MRI of Prostate Cancer: An Update on State-of- the-Art Techniques and Their Performance in Detecting and Localizing Prostate Cancer," *Ratio*, vol. 36, no. 3, pp. 490–499, 2010.

[21] R. Shimofusa *et al.*, "Diffusion-weighted imaging of prostate cancer," *J. Comput. Assist. Tomogr.*, vol. 29, no. 2, pp. 149–153, 2005.

[22] R. Bammer, "Basic principles of diffusion-weighted imaging," *Eur. J. Radiol.*, vol. 45, no. 3, pp. 169–184, 2003.

[23] "Advanced da Vinci Prostatectomy (Robotic Prostate Surgery) at CPMC San Francisco." [Online]. Available: http://www.cpmc.org/services/surgery/robotic/prostatectomy.html. [Accessed: 26-Mar-2017].

[24] C. M. Moore *et al.*, "Image-guided prostate biopsy using magnetic resonance imaging-derived targets: A systematic review," *Eur. Urol.*, vol. 63, no. 1, pp. 125–140, 2013.

[25] S. W. T. P. J. Heijmink, H. van Moerkerk, L. A. L. M. Kiemeney, J. A. Witjes, F. Frauscher, and J. O. Barentsz, "A comparison of the diagnostic performance of systematic versus ultrasound-guided biopsies of prostate cancer," *Eur. Radiol.*, vol. 16, no. 4, pp. 927–938, 2006.

[26] K. Eichler, S. Hempel, J. Wilby, L. Myers, L. M. Bachmann, and J. Kleijnen, "Diagnostic Value of Systematic Biopsy Methods in the Investigation of Prostate Cancer: A Systematic Review," *J. Urol.*, vol. 175, no. 5, pp. 1605–1612, 2006.

[27] M. Norberg, L. Egevad, L. Holmberg, P. Sparén, B. J. Norlén, and C. Busch, "The sextant protocol for ultrasound-guided core biopsies of the prostate underestimates the presence of cancer," *Urology*, vol. 50, no. 4, pp. 562–566, 1997.

[28] S. Y. Eskicorapci, F. Guliyev, E. Islamoglu, A. Ergen, and H. Ozen, "The effect of prior biopsy scheme on prostate cancer detection for repeat biopsy population: Results of the 14-core prostate biopsy technique," *Int. Urol. Nephrol.*, vol. 39, no. 1, pp. 189–195, 2007.

[29] A. De La Taille *et al.*, "Prospective evaluation of a 21-sample needle biopsy procedure designed to improve the prostate cancer detection rate," *Urology*, vol. 61, no. 6, pp. 1181–1186, 2003.

[30] B. J. Moran and M. H. Braccioforte, "Stereotactic Transperineal Prostate Biopsy,"

Urology, vol. 73, no. 2, pp. 386–388, 2009.

[31]   B. J. Moran, M. H. Braccioforte, and D. J. Conterato, "Re-biopsy of the Prostate Using a Stereotactic Transperineal Technique," *J. Urol.*, vol. 176, no. 4, pp. 1376–1381, 2006.

[32]   A. K. Leventis, S. F. Shariat, and T. Utsunomiya, "Characteristics of Normal ProstateVascular Anatomy as Displayed by Power Doppler," vol. 288, no. June 2000, 2001.

[33]   G. Kimura, T. Nishimura, R. Kimata, Y. Saito, and K. Yoshida, "Random systematic sextant biopsy versus power doppler ultrasound-guided target biopsy in the diagnosis of prostate cancer: positive rate and clinicopathological features.," *J. Nihon Med. Sch. = Nihon Ika Daigaku zasshi*, vol. 72, no. 5, pp. 262–269, 2005.

[34]   C. ROY, X. BUY, H. LANG, C. SAUSSINE, and D. JACQMIN, "Contrast Enhances Color Doppler Endorectal Sonography of Prostate: Efficiency for Detecting Peripheral Zone Tumors and Role for Biopsy Procedure," *J. Urol.*, vol. 170, no. 1, pp. 69–72, 2003.

[35]   A. Y. Hung, C. L. Amling, and F. V Coakley, "Direct MRI-guided biopsy of the prostate: use of post-biopsy needle track imaging to confirm targeting," vol. 40, no. 7, pp. 2517–2522, 2015.

[36]   I. G. Murphy, E. NiMhurchu, R. G. Gibney, and C. J. McMahon, "MRI-directed cognitive fusion-guided biopsy of the anterior prostate tumors," *Diagnostic Interv. Radiol.*, no. 12, 2017.

[37]   K. M. Pondman *et al.*, "MR-Guided Biopsy of the Prostate: An Overview of Techniques and a Systematic Review," *Eur. Urol.*, vol. 54, no. 3, pp. 517–527, 2008.

[38]   D. T. S. Chang, B. Challacombe, and N. Lawrentschuk, "Transperineal biopsy of the prostate--is this the future?," *Nat. Rev. Urol.*, vol. 10, no. 12, pp. 690–702, 2013.

[39]   J. Miller, C. Perumalla, and G. Heap, "Complications of transrectal versus transperineal prostate biopsy," *ANZ J. Surg.*, vol. 75, no. 1–2, pp. 48–50, 2005.

[40]   P. Emiliozzi, A. Corsetti, B. Tassi, G. Federico, M. Martini, and V. Pansadoro, "Best approach for prostate cancer detection: A prospective study on transperineal versus transrectal six-core prostate biopsy," *Urology*, vol. 61, no. 5, pp. 961–966, 2003.

[41]   R. Hara *et al.*, "Optimal Approach for Prostate Cancer Detection as Initial Biopsy: Prospective Randomized Study Comparing Transperineal Versus Transrectal Systematic 12-Core Biopsy," *Urology*, vol. 71, no. 2, pp. 191–195, 2008.

[42]   B. Nazir, "Pain during transrectal ultrasound-guided prostate biopsy and the role of periprostatic nerve block: What radiologists should know," *Korean J. Radiol.*, vol. 15, no. 5, pp. 543–553, 2014.

[43]   S. Loeb, H. B. Carter, S. I. Berndt, W. Ricker, and E. M. Schaeffer, "Complications after prostate biopsy: Data from SEER-Medicare," *J. Urol.*, vol. 186, no. 5, pp. 1830–1834, 2011.

[44]   R. K. Nam *et al.*, "Increasing Hospital Admission Rates for Urological Complications After Transrectal Ultrasound Guided Prostate Biopsy," *J. Urol.*, vol. 183, no. 3, pp. 963–969, 2010.

[45] W. Birkfellner, J. Hummel, and E. Wilson, "Tracking Devices," *Image-Guided Interv.*, pp. 23–45, 2008.

[46] J. Gempt *et al.*, "Frameless image-guided stereotaxy with real-time visual feedback for brain biopsy," *Acta Neurochir. (Wien).*, vol. 154, no. 9, pp. 1663–1667, 2012.

[47] N. L. Dorward, T. S. Paleologos, O. Alberti, and D. G. T. Thomas, "The advantages of frameless stereotactic biopsy over frame-based," vol. 16, no. January 2001, pp. 110–118, 2002.

[48] R. Dammers, I. K. Haitsma, J. W. Schouten, J. M. Kros, C. J. J. Avezaat, and A. J. P. E. Vincent, "Clinical Article Safety and efficacy of frameless and frame-based intracranial biopsy techniques," pp. 23–29, 2008.

[49] P. A. Pinto *et al.*, "Magnetic Resonance Imaging / Ultrasound Fusion Guided Prostate Biopsy Improves Cancer Detection Following Transrectal Ultrasound Biopsy and Correlates With Multiparametric Magnetic Resonance Imaging," *J. Urol.*, vol. 186, no. 4, pp. 1281–1285, 2011.

[50] W. J. M. Van De Ven, C. A. Hulsbergen-Van De Kaa, T. Hambrock, J. O. Barentsz, and H. J. Huisman, "Simulated required accuracy of image registration tools for targeting high-grade cancer components with prostate biopsies," *Eur. Radiol.*, vol. 23, no. 5, pp. 1401–1407, 2013.

[51] A. Faso, "Haptic and Virtual Reality Surgical Simulator for Training in Percutaneous Renal Access," UIC, 2017.

[52] C. Gatti, "Application of Haptic Virtual Fixtures in Psychomotor Skill Development for Robotic Surgical Training," UIC, 2017.

[53] E. Tagliabue, "Visuo-Haptic Model of Prostate Cancer Based on Magnetic Resonance Elastography," UIC, 2017.

[54] M. Bosi, "Visualization Library: Visualization Library Reference Documentation." [Online]. Available: http://visualizationlibrary.org/docs/2.0/html/index.html. [Accessed: 18-Apr-2017].

[55] "OpenGL." [Online]. Available: https://www.opengl.org/. [Accessed: 18-Apr-2017].

[56] "Ascension Technology Corp." [Online]. Available: https://www.ascension-tech.com/. [Accessed: 18-Apr-2017].

[57] "Medical Aurora." [Online]. Available: https://www.ndigital.com/medical/products/aurora/. [Accessed: 20-Nov-2017].

[58] "NDI C API." [Online]. Available: https://github.com/PlusToolkit/ndicapi. [Accessed: 20-Nov-2017].

[59] "OpenHaptic Toolkit Overview." [Online]. Available: http://www.geomagic.com/en/products/open-haptics/overview. [Accessed: 18-Apr-2017].

[60] "Wykobi Computational Geometry Library." [Online]. Available: http://www.wykobi.com/. [Accessed: 18-Apr-2017].

[61] "Clear Ballistics." [Online]. Available: https://www.clearballistics.com/. [Accessed: 20-Apr-2017].

[62] R. Amini, J. Z. Kartchner, L. A. Stolz, D. Biffar, A. J. Hamilton, and S. Adhikari, "A novel and inexpensive ballistic gel phantom for ultrasound training," vol. 6, no. 3, pp. 225–228, 2015.

[63] O. Sorkine-hornung and M. Rabinovich, "Least-Squares Rigid Motion Using SVD," no. 3, pp. 1–5, 2017.

[64] "Eigen: Main Page." [Online]. Available: http://eigen.tuxfamily.org/dox/. [Accessed: 18-Apr-2017].

[65] F. T. Luk and H. Park, "A Proof of Convergence for two Parallel Jacobi SVD Algorithms," *IEEE Trans. Comput.*, vol. 38, no. 6, pp. 806–811, 1989.

[66] L. Rapetti, S. Crivellaro, E. De Momi, G. Ferrigno, C. Niederberger, and C. Luciano, "Virtual Reality Navigation System for Prostate Biopsy," in *ACM Symposium on Virtual Reality Software and Technology*, 2017.

[67] L. Rapetti, "Virtual Reality Navigation System for Prostate Biopsy," UIC, 2017.